USGS
science for a changing world

Sources of Base Flow in the Upper Verde River

By Laurie Wirt

Chapter F

Geologic Framework of Aquifer Units and Ground-Water Flowpaths, Verde River Headwaters, North-Central Arizona

Edited by Laurie Wirt, Ed DeWitt, and V.E. Langenheim

Prepared in cooperation with the Arizona Water Protection Fund Commission

Open-File Report 2004–1411-F

U.S. Department of the Interior
U.S. Geological Survey

U.S. Department of the Interior
Gale A. Norton, Secretary

U.S. Geological Survey
P. Patrick Leahy, Acting Director

U.S. Geological Survey, Reston, Virginia: 2005

For product and ordering information:
World Wide Web: http://www.usgs.gov/pubprod
Telephone: 1-888-ASK-USGS

For more information on the USGS--the Federal source for science about the Earth, its natural and living resources, natural hazards, and the environment:
World Wide Web: http://www.usgs.gov
Telephone: 1-888-ASK-USGS

Suggested citation:
Wirt, L., 2005, Sources of Base Flow in the Upper Verde River: *in* Wirt, Laurie, DeWitt, Ed, and Langenheim, V.E., eds., Geologic Framework of Aquifer Units and Ground-Water Flowpaths, Verde River Headwaters, North-Central Arizona: U.S. Geological Survey Open-File Report 2004-1411-F, 34 p.

Contents

Figures

Tables

Sources of Base Flow in the Upper Verde River

By Laurie Wirt

Abstract

Base flow in the upper Verde River begins downgradient from Big and Little Chino valleys and the regional carbonate aquifer in three different locations—Stillman Lake, lower Granite Creek, and upper Verde River springs. The relative contribution of inflow from each of three aquifer sources is difficult to directly measure because most of the inflows occur diffusely through the streambed. A tracer-dilution study and synoptic water-chemistry sampling were conducted during low-flow conditions to identify locations of inflows and to determine the relative contribution from major aquifers. Discharge was determined using the analytical concentration of chloride tracer to calculate dilution. Ground-water inflows produced spatial trends in field parameters, major and trace elements, and stable isotopes of hydrogen and oxygen. Last, inverse modeling was used to constrain hypotheses regarding the nature of water-rock interactions and to determine the extent of mixing along the flowpath between the Big Chino aquifer near Paulden and upper Verde River springs.

Base flow at Stewart Ranch was 19.5±1.0 ft^3/s, compared with 21.2±1.0 ft^3/s downstream at the Paulden gauge during the same time interval. By subtraction, approximately 7 percent of base flow at the Paulden gauge was contributed downstream from the tracer reach, with some inflows observed in the vicinity of Muldoon Canyon. The Little Chino basin-fill aquifer contributed 2.7±0.08 ft^3/s, or 13.8±0.7 percent, with upper Verde River springs contributing the remaining 86.2 percent of total base flow at Stewart Ranch. Most of the Little Chino inflow was derived from the Stillman Lake flowpath, as opposed to lower Granite Creek.

Inverse model simulations using the geochemical computer program PHREEQC indicate that discharge to upper Verde River springs upstream from Stewart Ranch is predominantly derived from a mixture of initial water types within lower Big Chino Valley. A small amount of mixing with the Mississippian-Devonian (M-D) sequence north of the Verde River is plausible, although none is required to account for the observed water chemistry. About 10 to 15 percent of discharge to upper Verde River springs is attributed to ground water from the Devonian-Cambrian (D-C) zone of the carbonate aquifer underlying and adjoining the Big Chino basin-fill aquifer near Paulden. Important reactions along the Big Chino basin outlet flowpath include the dissolution of silicate minerals and degassing of carbon dioxide. Despite extensive contact with limestone, dissolution of carbonate minerals does not appear to be a dominant process along the outlet flowpath. Adjusted contributions from each aquifer source to base flow at the Paulden gauge are estimated as: (a) Little Chino basin-fill aquifer, 14 percent; (b) M-D sequence north of the Verde River, less than about 6 percent; and (c) the combined Big Chino basin-fill aquifer and underlying D-C zone of the carbonate aquifer, at least 80 to 85 percent.

Introduction

Perennial base flow in the upper Verde River begins downgradient from three aquifers—the Big and Little Chino basin-fill aquifers and the carbonate aquifer north of the Verde River (Mississippian-Devonian, or M-D sequence). Base flow is defined as the sustained low-flow condition of a stream and is derived from ground-water inflow to the stream channel, in contrast to runoff from rainfall or snowmelt. Base flow emerges in three locations in the vicinity of the confluence of Granite Creek and the Verde River, including (a) Stillman Lake, (b) the cienaga in lower Granite Creek referred to in this report as "Lower Granite spring," and (c) the gaining reach of the Verde River channel downstream from river mi 2.2, referred to here as "upper Verde River springs." Because the inflows occur diffusely and the precise points of discharge are not always evident, the inflows are difficult to measure directly using a traditional current-meter approach. Consequently, the relative contribution and source(s) of the various inflows (particularly the M-D sequence of the carbonate aquifer) previously have not been well understood, allowing for conflicting interpretations.

Daily mean flow at the U.S. Geological Survey (USGS) streamflow gauging station near Paulden (09503700), which is referred to in this report as the "Paulden gauge" (fig. F1), is about 25 cubic ft per second (ft^3/s) (1964 through 2003 water years, Fisk and others, 2004). Historically, perennial base flow in the upper Verde River was greater than it is now and began at Del Rio Springs (Wirt, Chapter A, this volume). At present, the first perennial segment of base flow in the Verde River is an impounded reach of river channel intercepting the water table, informally known as Stillman Lake (between river mi 1.0 and 2.0, fig. F1). The lake is dammed by a low levee of stream-deposited sediment upstream from

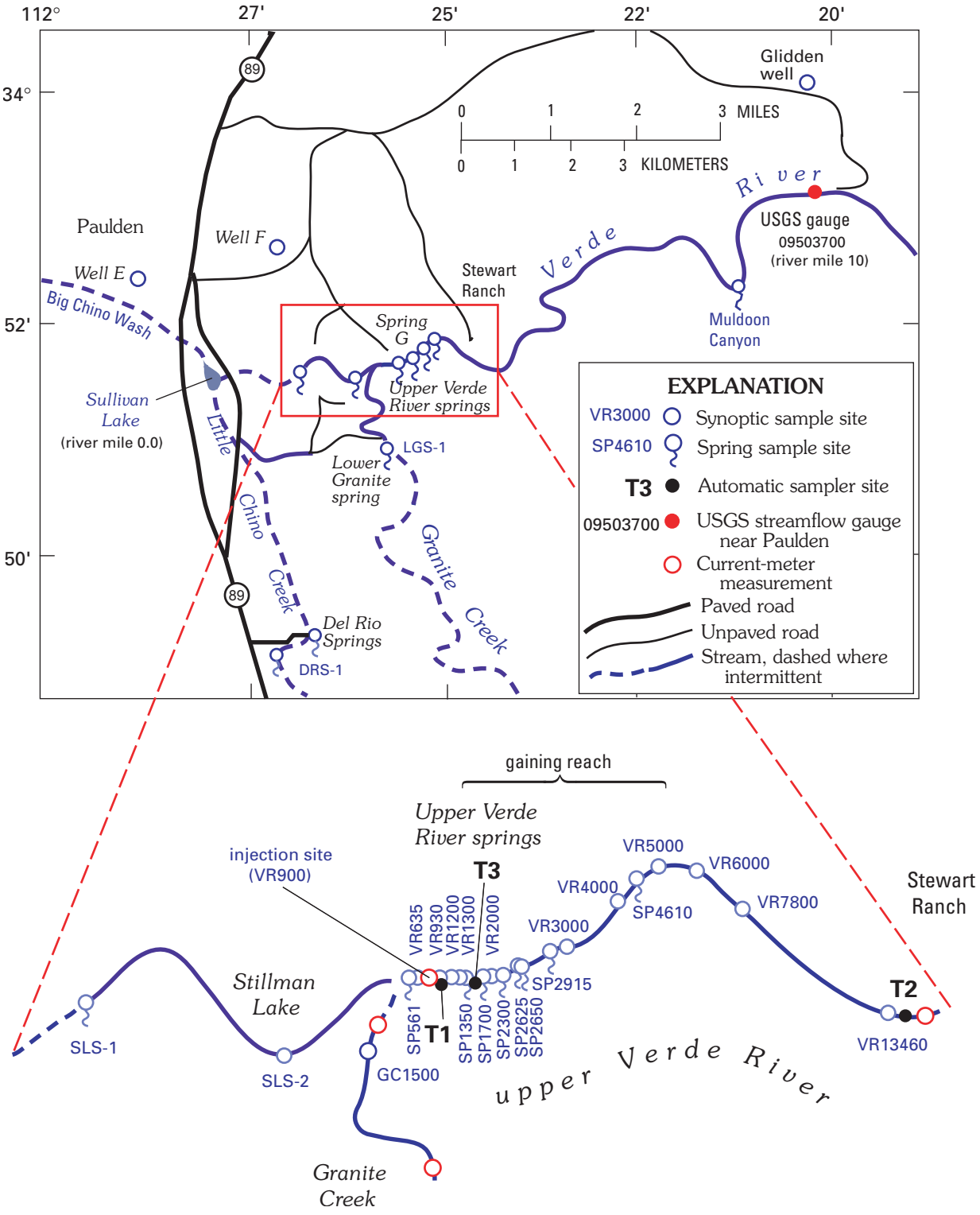

Figure F1. Map showing location of tracer-dilution sampling locations, upper Verde River, north-central Arizona.

the mouth of Granite Creek (fig. F2). A second point of perennial flow begins in lower Granite Creek. In June 2000, base flow in the lowermost mi of Granite Creek peaked at about 0.5 ft^3/s before seeping into the stream alluvium near its confluence. As interpreted from stable-isotope data and strontium concentrations (Wirt and DeWitt, Chapter E, this volume) and water-level gradients (Wirt and others, Chapter D, this volume), the source of ground water discharging to Stillman Lake and lower Granite Creek is the Little Chino basin-fill aquifer. Below its confluence with Granite Creek, the Verde River was dry for more than more than 600 ft until flow reemerged as a cienaga (fig. F3A). Underflow from Stillman Lake and lower Granite Creek flowed beneath the ephemeral reach, discharging to the upper Verde River near site VR635 (fig. F1).

Downstream from site VR635, base flow in the upper Verde River was permanent and continuous, increasing to about 19 ft^3/s within the next mi. Most of the gain came from a large, diffuse spring network discharging from the Martin Limestone near river mi 2.2, formerly referred to as "Big Chino Springs" (Wirt and Hjalmarson, 2000) and here as "upper Verde River springs." Since 2000, beavers have intermittently dammed the Verde River near upper Verde River springs, creating a series of ponds and flooding the major spring outlet (fig. F3). Wirt and DeWitt (Chapter E, this volume) have shown that the water chemistry of upper Verde River springs is consistent with ground water from the Big Chino basin-fill aquifer that has been in contact with rocks in the Devonian Cambrian zone (D-C zone) of the carbonate aquifer. The D-C zone underlies lower Big Chino Valley and also lies between Big Chino Valley and upper Verde River springs. As demonstrated by water-level data (Wirt and others, Chapter D, this volume), the two aquifers are strongly interconnected at the ground-water outlet of the Big Chino basin-fill aquifer near Paulden. An unknown fraction of ground water from the M-D sequence of the carbonate aquifer north of the upper Verde River has been hypothesized to mix with Big Chino ground water before discharging to upper Verde River springs.

Estimates of the relative contribution from the Big Chino basin-fill aquifer to the upper Verde River have been an ongoing source of controversy (Hendrickson, 2000; Dodder, 2004). Wirt and Hjalmarson (2000) estimated that at least 80 percent of the base flow to the upper Verde River springs (formerly referred to as Big Chino Springs) was derived from the Big Chino basin-fill aquifer, with the remaining fraction largely attributed to the Little Chino basin-fill aquifer. Their estimate was based on two independent lines of evidence, namely (1) a mass-balance calculation using $\delta^{18}O$ data from a 1991 seepage study (Ewing and others, 1994), and (2) a water-budget approach based on historical base-flow, precipitation, water-level, and water-use data. A separate contribution from the regional carbonate aquifer was not considered because the regional flow gradients were consistent with this interpretation. In addition, there was little water-chemistry information

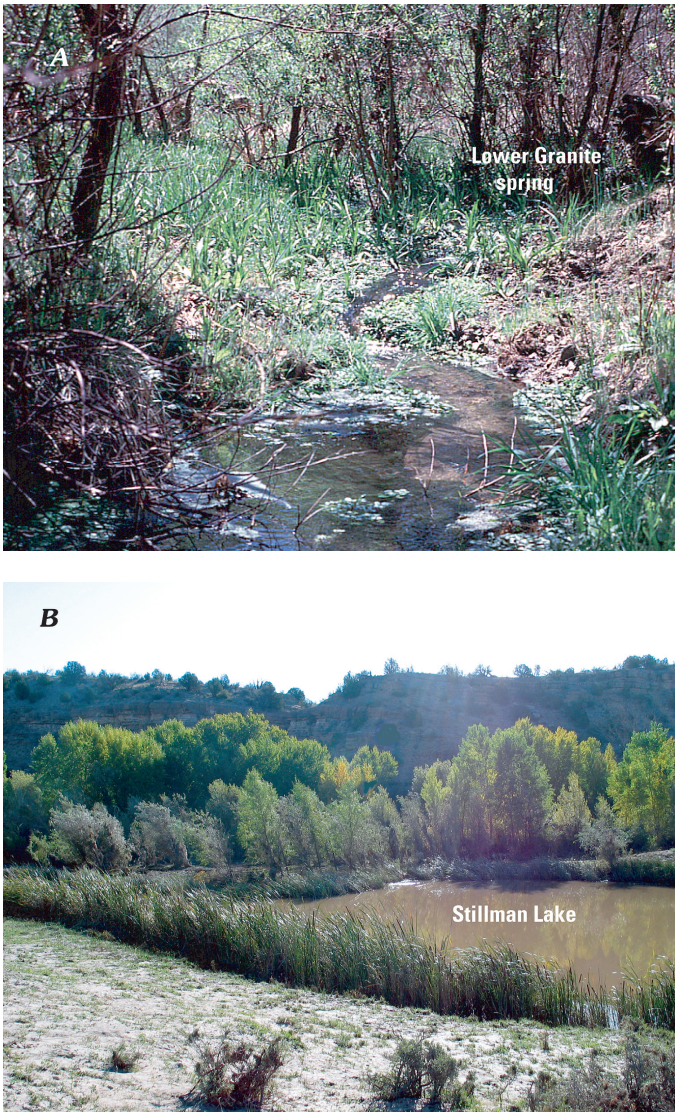

Figure F2. Photographs showing sources of perennial flow in the upper Verde River at (*A*) Lower Granite spring, emerging through stream channel one mile upstream from mouth of Granite Creek, and (*B*) lower end of Stillman Lake showing cattail marsh and natural sediment levee. Photographs by Laurie Wirt and Charles Paradzick of the Arizona Game and Fish Department.

available north of the Verde River at the time of that study. In contrast, Knauth and Greenbie (1997) concluded that the major source of discharge to the upper Verde River was the carbonate aquifer north of the upper Verde River. Their interpretation was largely based on similarities between a few samples collected from the upper Verde River and the Glidden well (fig. F1) and the observation that most of the springs in the river canyon emerge from limestone. Subsequent sampling has shown that the stable-isotope results

from the regional carbonate aquifer north of the upper Verde River are more depleted and more variable than those for upper Verde River springs, which more closely resembles the chemistry of ground water at the Big Chino basin outlet near Paulden (Chapter E, this volume, fig. E5). The different conclusions reached by the two studies illustrates that although stable isotopes are useful natural tracers of water sources, a reliance on too few stable-isotope results in the absence of other supporting evidence sometimes will lead to an interpretation that is biased by the low number of samples, a limited distribution of samples, or one that does not fully reflect the full range of possible scenarios.

The goal of this chapter is to more precisely determine the contributions from each aquifer (as opposed to the contributions from a geographical area) to the upper Verde River. At the end of Chapter A in this report, an estimate of the relative contributions from each aquifer to base flow of the upper Verde River was compiled from the results of earlier studies (fig. A16, Chapter A, this volume). This simple water-budget approach suggests that the combined aquifers beneath Big Chino Valley and Big Black Mesa presently contribute about 92 percent of base flow at the Paulden gauge; Little Chino Valley contributes the remainder. Because the budget was compiled from several studies using various approaches, no precision or accuracy could be assigned to this working model. In addition, little information was available for the regional carbonate aquifer north of the upper Verde River between Big Black Mesa and Hell Canyon. This chapter will draw on the geologic and geophysical framework results (Chapters B and C, this volume), the hydrogeology (Chapter D, this volume), and geochemistry data for major aquifers and springs (Chapter E, this volume), to constrain flowpaths and quantify the contribution from specific aquifer units.

In this chapter, synoptic sampling and a tracer-dilution study provide more detailed spatial coverage than earlier studies by Knauth and Greenbie (1997) and Wirt and Hjalmarson (2000). Spatial trends in pH, specific conductance, temperature, major and trace elements, and stable isotopes are evaluated with distance along the gaining reach of the upper Verde River to identify trends (fig. F1). Next, inverse modeling using PHREEQC (Parkhurst and Appelo, 1999) is used to identify major geochemical processes occurring between the Big Chino basin-fill aquifer and the upper Verde River and to determine the degree of potential mixing with the regional carbonate aquifer. The geochemical modeling helps to integrate multiple lines of geochemical evidence and reduce the number of viable nonunique interpretations. Mass-balance estimates of mixing fractions identified by PHREEQC do not rely solely on stable-isotope data to the exclusion of other geochemical results, a problem with earlier interpretations. Moreover, the model results are interpreted in context with the geologic framework and geochemical processes that have been identified along the outlet flowpath.

Purpose and Scope

The objectives of this study are to determine locations of ground-water inflows to the uppermost gaining reach of the Verde River and to quantify the relative contributions from each of the three major aquifers to base flow at Stewart Ranch. The tracer-dilution method (Kimball, 1997; Bencala and others, 1990; Broshears and others, 1993; Kimball and others, 1994) was used to locate and quantify inflows from springs discharging to the Verde River between the mouth of Granite Creek and Stewart Ranch (fig. F1). The study was conducted during low-flow conditions from June 15 to 19, 2000, which is now considered a period of extended drought (Betancourt, 2003). Field reconnaissance measurements of pH, specific conductance, and dissolved oxygen were used to select water-chemistry sampling sites. Multiple lines of geochemical evidence (field parameters, major and trace elements, and stable-isotopes of oxygen and hydrogen) are presented to characterize the inflows, identify their source(s), and indicate where mixing is occurring. Finally, inverse modeling of water-chemistry analyses along the major flowpath from Paulden to upper Verde River springs is used to determine major geochemical processes and the degree of mixing with the M-D sequence.

In this study, the rate of discharge (volume of fluid passing a point per unit of time) was determined using a dilution approach by continuously injecting a saturated sodium-chloride (NaCl) solution into the beginning of the reach until steady-state mixing had occurred throughout, followed by synoptic sampling. In a synoptic study, many discharge measurements are made within a short period, providing a "snapshot" in time. Once the tracer solution reached steady-state conditions, twelve flow-weighted streamflow synoptic samples were collected from a 2-mi reach of the upper Verde River within a 1-hour timeframe. In addition, twelve ground-water inflows were collected from discrete spring inflows along the upper Verde River, from the perennial reach of lower Granite Creek, and from different parts of Stillman Lake over a 3- day timeframe, for a total of 24 water-chemistry samples.

Characterization of the water chemistry of spring inflow data from the synoptic sampling presented in this chapter relies on the characterization of water chemistry of major aquifers, recharge areas, and springs presented earlier in Chapter E (this volume). Chapter E provides a detailed discussion of the water chemistry of the Big and Little Chino basin-fill aquifers as well as that of different areas within the carbonate aquifer. As in Chapter E, the regional carbonate aquifer within the Transition Zone geologic province is subdivided into the Mississippian-Devonian (M-D) sequence north of the upper Verde River and the Devonian-Cambrian (D-C) zone underlying the Big Chino basin-fill aquifer near Paulden. The four D-C zone samples, which are located along the fault-bounded margin of the Big Chino basin-fill aquifer (fig. E1, Chapter E, this volume), do not necessarily represent the water chemistry of the carbonate aquifer underlying the Big Chino basin-fill

aquifer in the middle of Big Chino Valley. The underlying carbonate aquifer is largely unsampled.

Acknowledgments

This study was funded by the Arizona Water Protection Fund. Land access was granted by the Prescott National Forest and the Arizona Department of Game and Fish. The following local residents graciously granted permission for water-sampling activities: Billy Wells, Harley and Patty Shaw, and Ann Harrington. Field support was provided by David Christiana of the Arizona Department of Water Resources and by Tasha Lewis and Steve Acquafredda of the Department of Hydrology and Water Resources at the University of Arizona. USGS personnel who assisted the author in the field include Ken Leib, Jonathan Evans, Betsy Woodhouse, Owen Baynham, Bert Duet, and Ken Fossum. Most of all, the author is indebted to Pierre Glynn of the USGS for his help with PHREEQC and inverse modeling.

Environmental Setting and Base-Flow Conditions

Base flow in the upper Verde River begins in three locations—at Stillman Lake, Lower Granite spring, and upper Verde River springs (figs. F1–A3). The geologic setting is a narrow canyon incised up to 250 ft in depth into Paleozoic sedimentary rocks and, in some places, Tertiary basalt. Most Paleozoic carbonate rocks and the Tertiary basalt have moderate to high permeability (Wirt and others, Chapter D, table D1). The Martin Limestone (Devonian) contains abundant northwest-striking high-angle joints near its base, which enhance its overall permeability. Locally, the Martin contains dissolution cavities and other small karst features. The bottom contact of the Martin Limestone is a stratigraphic nonconformity with the underlying Chino Valley Formation (where present) or Tapeats Sandstone. The Tapeats Sandstone (Cambrian) has low permeability, due to its strongly cemented nature. The Chino Valley Formation (Cambrian?), found above the Tapeats, has three units consisting of a lithic sandstone, a pebble conglomerate, and a red shaley dolomite. The Chino Valley is inferred to have low porosity owing to the high clay content of the shale (Chapter D, this volume), but its actual permeability is unknown.

Stillman Lake is an impounded section of channel between river mi 1.0 and 2.0 (fig. F1). The lake is less than 5 ft in depth. The downstream end of the lake terminates in a cattail marsh above the mouth of Granite Creek (fig. F2B and cover photograph). This mile-long curving channel receives occasional runoff whenever runoff overtops the dam at Sullivan Lake during large floods (Chapter A, this volume, fig. A13). The primary source of water in Stillman Lake, however, is ground water rather than surface water. The water level of Stillman Lake varies little between storm runoff events because it intersects the water table (Wirt and others, Chapter D, this volume, fig. D8). Stillman Lake is fed by ground water from the Little Chino basin-fill aquifer. The lake water has undergone evaporation, based on the enrichment of the stable isotopes of oxygen and hydrogen (Wirt and DeWitt, Chapter E, this volume, fig. E4).

During this study, the upper Verde River was in the third year of a drought and little if any rainfall runoff had overtopped the dam at Sullivan Lake for more than a year (Tadayon and others, 2000 and 2001; MacCormack and others, 2002). The 2000 water year had an annual mean discharge of 22.5 ft^3/s at the Paulden gauge (16,370 acre-ft/yr), which is the lowest annual discharge on record, as of this writing (MacCormack and others, 2002). This compares closely with the mean base flow of 16,000 acre-ft/yr calculated by Freethey and Anderson (1986) and 18,000 acre-ft/yr calculated by Wirt and Hjalmarson (2000). Both of these earlier studies estimated base flow using a hydrograph separation approach, but for differing time periods of record at the Paulden gauge. Because no runoff occurred in the 2000 water year, hydrograph separation is not required to estimate annual base flow.

A long, straight segment of the lake coincides with what Krieger (1965, pl. 2) mapped as a fault offsetting the Martin Limestone and Tapeats Sandstone or with what may instead be a unconformity between the Martin and Chino Valley Formation. Detailed field mapping is needed to determine the precise nature of this contact. Near the mouth of Granite Creek, the Chino Valley is a slope-forming unit that consists of thin alternating layers of sandstone, conglomerate, and a shaley dolomite (Hereford, 1975). Before being recognized as a separate unit, the Chino Valley was mapped as part of the Tapeats by Krieger (1965). The Chino Valley Formation, where present, lies between the Tapeats and the Martin.

Perennial flow in lower Granite Creek emerges from the stream channel about 1 mi upstream from the mouth near two small faults in the lower Paleozoic strata (Krieger, 1965, Plate 2). The spring is shown on U.S. Geological topography maps and is referred to informally in this report as “Lower Granite spring” or site LGS-1 (figs. F1–F2). Several large cottonwood trees grow west of the spring in a low-lying area between the two faults, indicating a high water table. Also, a large cottonwood tree grows east of the spring along the same trend, suggesting preferred availablility of ground water along this orientation. Based on the geochemical evidence, the source of base flow in Granite Creek (as well as Stillman Lake) has been linked to the Little Chino basin-fill aquifer (Wirt and DeWitt, Chapter E, this volume). Parts of lower Granite Creek are a cienaga. Base flow in lower Granite Creek has been measured at 0.55 ft^3/s in 1977 (Owen-Joyce and Bell, 1983), estimated at <0.5 ft^3/s in 1991 (Boner and others, 1991, Ewing and others, 1994), and measured by Parshall flume at 0.13 ft^3/s in 1996 (Knauth and Greenbie 1997). These data were collected by different parties at different times and locations. In this study, the flow in lower Granite Creek was measured twice at 0.5 ft^3/s in two different locations. The quantity of underflow through alluvium flowing beneath lower Granite Creek is unknown, but probably is small because bedrock is shallow.

Base flow in lower Granite Creek varies substantially in response to seasonal and temporal changes. In June 2000, diurnal changes in flow were relatively large owing to the small amount of stream discharge and large degree of evapotranspiration. In gaining and losing segments, much of the streamflow disappeared entirely during the heat of the day and reappeared at night and through the early morning. This especially was the case near its confluence with the Verde River canyon, which is a losing reach. Here, the precise point where streamflow disappeared into the loose, sandy gravel moved up and down the alluvial channel above the mouth of Granite Creek by more than 50 ft over the course of the day. During the cooler months, perennial flow in Granite Creek was considerably greater than in the summer and typically extended beyond the confluence to join perennial flow in the upper Verde River below Stillman Lake—presumably, in part, because riparian plants are less active during the winter, and less water is lost to evapotranspiration.

Downstream from the mouth of Granite Creek, the upper Verde River was dry throughout 1999–2001. In June 2000, the dry reach of the upper Verde River below the confluence extended 560 ft downstream from the natural sediment levee below Stillman Lake. From mi 2.1 onward, flow in the Verde River was permanent and continuous. Discharge increased to about 19 cubic ft per second (ft^3/s) before reaching Stewart Ranch (Knauth and Greenbie, 1997; Wirt and Hjalmarson, 2000; and this study). Most of the gain occurred downstream from a large, unnamed spring (site SP1700; fig. F3B) that emerged on the north bank through Martin Limestone. Much of the inflow occurred diffusely through the streambed and could not be sampled directly.

Base flow in the upper Verde River, as in lower Granite Creek, is strongly influenced by evapotranspiration. During the tracer experiment, daily discharge at the USGS streamflow-gauging station near Paulden (station number 09503700; river mi 10) ranged from 19 to 21 ft^3/s with a diurnal range of 2 ft^3/s, or ten percent of the maximum daily flow occurring about every 12 hours (fig. F4). The daily peak at the Paulden gauge occurred each morning between 0400 and 1200 hours, based on pressure-transducer recordings at 15-minute intervals. The lowest discharge occurred between 1600 and 2400 hours in the evening. The timing of the peak and trough at the Paulden gauge lags a few hours behind what was observed 6 to 8 mi upstream in the study reach.

Near site VR635 at the beginning of the study reach (fig. F1), the highest observed flows occurred around daybreak (before 0700 AM) and the lowest flows were observed in the late afternoon following the hottest part of the day (after about 1700 PM until midnight). At daybreak, streamflow began more than 60 ft upstream from site VR635 near site VR561 and the discharge was visibly greater than that observed later in the day. Similarly, the flow in lower Granite Creek extended about 50 ft further downstream towards the confluence with the upper Verde River canyon in the morning than it did in the afternoon. These observations correspond with air temperature and photosynthesis activity of riparian vegetation along the stream corridor. Based on these field observations, it was evident that synoptic samples needed to be collected as quickly as possible in order to minimize effects of diurnal changes in base flow.

Figure F3. Photographs of upper Verde River gaining reach (*A*) site of tracer injection (VR900) on June 15, 2000, and (*B*) beaver dam near inflow from large spring (SP1700) emerging in right foreground (north bank), taken in 2004. Most ground-water inflows are diffuse and emerge through the streambed or are hidden by dense vegetation on either bank. Photographs by David Christiana and Charles Paradzick, respectively.

The degree of evapotranspiration is related to the amount of upstream riparian vegetation at any given point along the stream. In general, the canyon and floodplain are narrow and the vegetation consisted of willow, cottonwood, mesquite, and mixed broadleaf plants (figs. F2 and F3). Using the integration method, Anderson (1976) calculated the annual consumptive

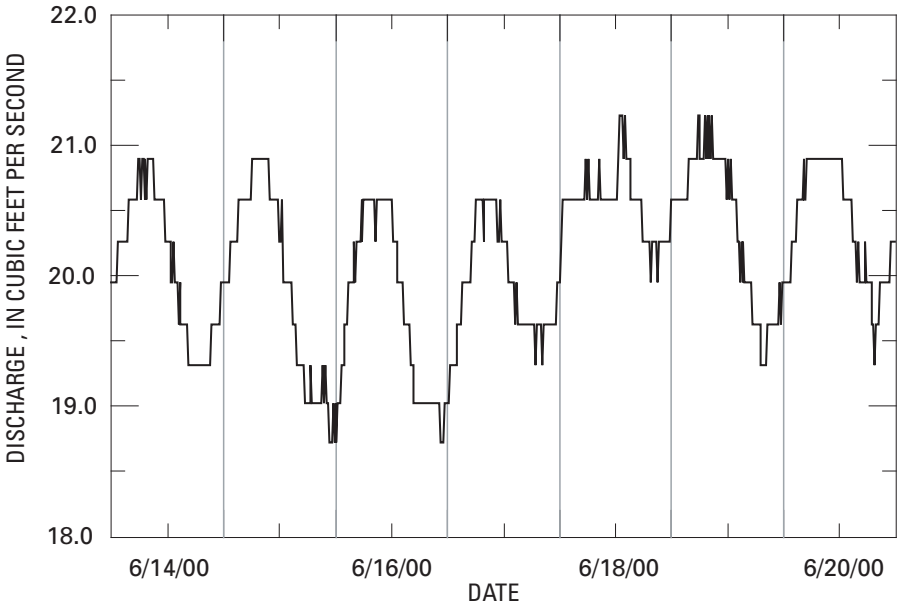

Figure F4. Graph showing diurnal variation in discharge at the USGS streamflow-gauging station near Paulden, Arizona, (09503700) near river mile 10 on June 14–20, 2000 (U.S. Geological Survey, 2000). Pressure-transducer data recorded every 15 minutes (ft^3/s). Peak of diurnal flow occurred between 0400 and 1200 AM. Trough occurred between 1600 and 2400 PM.

use by riparian vegetation upstream from the Paulden gauge to be 600 acre-ft/yr over an area of 384 acres. This is equivalent to an average of 2.2 acre-ft per acre. Based on field observations, the occurrence of riparian vegetation and aquatic plants was denser in gaining reaches than in non-gaining reaches. For example, the presence of algal strands and nonnative watercress growing on stream substrate was an excellent indicator of spring flow. Also, the wet part of the stream tended to be wider in marshy areas having seepage. From year to year, the density of trees and vegetation probably changes as a consequence of damage from large floods and beaver activity. Changes in vegetation could have a measurable effect on the amount of base flow lost to evapotranspiration.

Methods and Approach

Discharge by Tracer-Dilution Method

Dilution of a continuously injected chemical tracer provides a more accurate means to measure discharge than other methods in less-than-ideal stream cross sections. Current-meter measurements work well where the channel bottom and banks are smooth. They tend to be less accurate where the channel is irregular owing to large boulders or thick aquatic vegetation, or where a large fraction of flow moves beneath the stream through what is known as the hyporheic zone (Bencala and others, 1990). Traditional measurements of discharge can thus miss a substantial percentage of the flow (Kimball, 1997; Kimball and others, 2000). In the upper Verde River, the marshy banks and vegetated stream bottom create wide, shallow cross sections with numerous obstructions, making it difficult to accurately measure flow using a current meter. Hyporheic flow probably is not an important issue within a gaining reach but could be important in other nongaining reaches further downstream. Another advantage of the tracer method is that synoptic samples can be collected much faster than it takes to complete the same number of current-meter measurements, allowing many discharge estimates to be made in a short timeframe over a long reach.

The choice of tracer generally is limited to anions (which tend to stay in solution) such as chloride, bromide, and sulfate, and to some organic dyes (Zellweger, 1996). Chloride was chosen for the tracer based on presynoptic data for the upper Verde River indicating that natural levels of chloride were low and varied little over the stream reach (Boner and others, 1991). Chloride is nontoxic and has little effect on the stream environment at low concentrations. Ninety-nine percent pure NaCl, obtained locally in a 50-lb sack as stock salt, was used to make the tracer solution because it was inexpensive and locally available.

In the tracer-dilution approach, discharge is determined by adding a known quantity of salt tracer, such as NaCl, to a stream. Discharge is calculated by measuring the amount of dilution that occurs as the tracer moves downstream (Kimball, 1997). This technique is illustrated in figure F5 and described by the following mass-balance equation:

$$Q_S = \left(\frac{C_{INJ} Q_{INJ}}{C_B - C_A} \right) \quad (1)$$

where:

Q_s = stream discharge, in cubic ft per second;
C_{INJ} = tracer concentration in the injection solution, in mg/L;
Q_{INJ} = rate of tracer injection to the stream, in cubic ft per second;
C_B = tracer concentration downstream from injection point, in mg/L; and
C_A = tracer concentration upstream from injection point, in mg/L.

Streamflow discharge can be calculated at any site downstream from the injection site by using the instream tracer concentration and the concentration and injection rate of the tracer. Adjustment was made for the changes in chloride concentration from major sampled inflows as follows:

$$Q_F = Q_D \left(\frac{C_D - C_E}{C_F - C_E} \right) \quad (2)$$

where:

Q_F = stream discharge downstream from ground-water inflow, in cubic ft per second;
Q_D = stream discharge upstream from ground-water inflow, in cubic ft per second;
C_D = in-stream concentration of chloride upstream from ground-water inflow, in mg/L;
C_E = background concentration of chloride of ground-water inflow, in mg/L; and
C_F = in-stream concentration of chloride downstream from ground-water inflow, in mg/L.

Inflows include visible spring inflows that can be sampled directly and diffuse seeps in the form of ground-water discharge through the streambed that cannot be sampled directly. The magnitude of each inflow can be determined by the difference in streamflow between the mainstem sites immediately downstream and upstream from the inflow. Corrections were made for the background chloride in unsampled inflows by adjusting for sampled inflows upstream and downstream from diffuse inflows. The term "background" refers here to the amount of chloride that occurs naturally in local ground water (see fig. E3, Chapter E, this volume).

The dilution method assumes that mixing of the tracer is rapid and uniform, that the behavior of the tracer is conservative, that no stream losses occur, and that background chloride concentrations from tributaries and inflows are less than the injected tracer concentrations. The term "conservative" is used to describe elements that are unlikely to undergo geochemical reactions or sorption. The method works best when conditions are constant or steady state; however, the method still can be applied when discharge is rising or falling—such as from diurnal changes in evapotranspiration, or runoff events from storms—if all tracer-dilution samples are obtained within a short timeframe by synoptic sampling. Synoptic samples are collected using flow-weighted sampling protocol (Shelton, 1994), to further ensure that tracer concentrations are representative of well-mixed conditions.

Field Reconnaissance

In the 2 days preceding the synoptic sampling, detailed field reconnaissance was conducted in order to select the synoptic water-chemistry sample sites (fig. F1). The study benchmark was located at the natural sediment dam at the lower end of Stillman Lake. All taped distances were measured relative to this point. The study reach was measured and flagged by stretching a 200-ft tape measure along the thalweg or center of the stream. Latitude and longitude locations were determined by using a hand-held global positioning system (GPS); however, the steepness of the canyon walls limited the accuracy of those horizontal measurements to within 50 ft. Consequently, taped distances were deemed more accurate.

Field parameters were measured at 100–200 ft intervals in the first 2,200 ft below the benchmark and at 1,000–2,000 ft intervals thereafter (table F1). The greater frequency of measurements in the upper part of the tracer reach corresponds with the area having the greatest gain in discharge. Station numbers were assigned according to the taped distance downstream from the downstream end of Stillman Lake and the type of site. For example, site VR635 (which is the first point of seepage on the Verde River) is 635 ft downstream from the study benchmark at the center of the natural dam at Stillman Lake. Similarly, site SP1700 is a discrete spring outside the flowing river channel that is 1,700 ft downstream from the study benchmark.

Synoptic sample sites were chosen to bracket known springs in order to obtain discharge values above and below each inflow and to closely bracket unobserved inflows in the gaining reach. In reaches where no visible inflows were present, changes in pH, water temperature, specific conductance, and dissolved oxygen data were used as guides for selecting sample sites. These field reconnaissance measurements are presented in the "Results" section. Most discrete spring samples in the study reach were collected and processed immediately following the synoptic sampling. Samples from major springs and tributaries did not have to be collected at precisely the same time as the synoptic stream sampling because the water chemistry of these inflows was not potentially affected

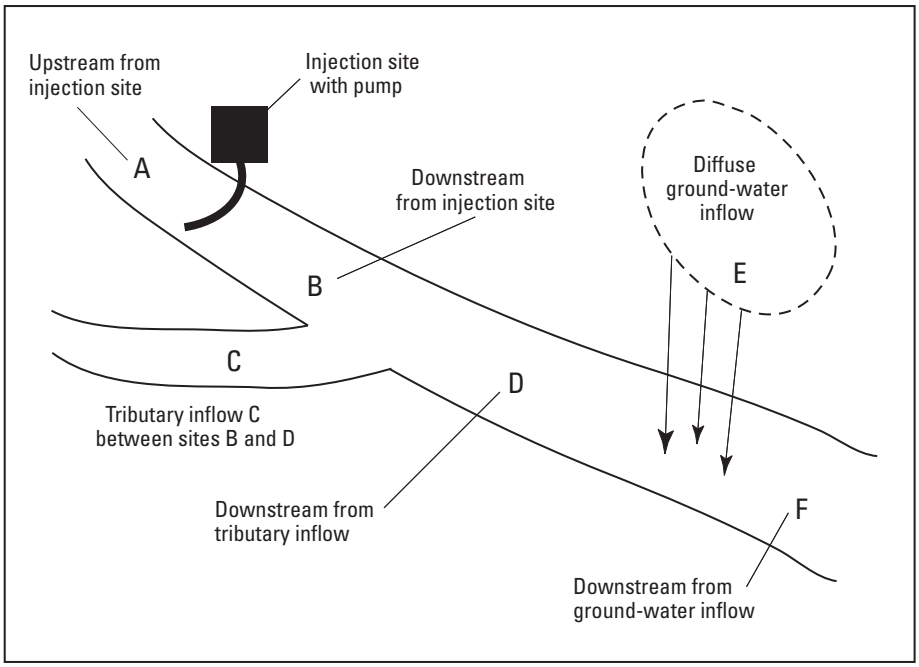

Figure F5. Schematic diagram showing mass-balance calculations in a gaining reach of stream with tributary and diffuse ground-water inflows. Diagram modified from Kimball and others (2000) to illustrate equations 1.0 and 2.0.

by diurnal variations in instream mixing. Samples from Del Rio Springs, Granite Creek, and Stillman Lake were collected from June 15–17, 2000.

After the injection of tracer solution had started, an ion-selective chloride probe was used to monitor relative changes in the tracer concentration with distance along the study reach (fig. F6). The relative potential is measured by the probe in millivolts and the value is inversely proportional to the amount of chloride present. Results from the selective-ion probe were used to determine the arrival time of the tracer at the end of the reach and to evaluate the degree of mixing of the tracer with distance through the reach. In addition, stream velocities were measured in the study reach by current meter. These values, ranging between 0.5 and 1.5 ft/s, also helped to predict arrival times of the tracer at the lower end of the reach.

The data from the selective ion probe were not used to calculate discharge because the analytical approach is more accurate for this purpose. The relative chloride potential measurements indicated rapid dilution of the chloride tracer between the injection point and site VR2000 before stabilizing within a narrow range (fig. F6). Because measurements were made at different times during the day, the variation in relative chloride potential values between sites VR6000 and VR13460 (fig. F1) is attributed largely to diurnal variations in flow. The reconnaissance measurements were collected by two teams over a 2-day period. Graphing these data in the field assisted in selection of synoptic sample sites.

Field Activities and Equipment

Field activities and equipment described in this section include (a) continuous gauge readings and current-meter measurements, (b) the setup and operation of tracer injection equipment, (c) the setup and application of automatic samplers, and (d) synoptic sampling.

Gauge Readings and Current-Meter Measurements

Stage readings at the Paulden gauge and manual current-meter measurements provided a means to estimate the concentration of tracer needed, as well as an independent cross check of discharge determined by tracer dilution. Although 6 mi downstream from Stewart Ranch, readings from the Paulden gauge helped to predict the timing and range of diurnal fluctuations. Discharge in the study reach was measured using an AA current meter as described by Rantz and others (1982a and 1982b). In order to improve the accuracy of the current-meter measurements, the cross-sectional shape of the channel was improved by removing aquatic vegetation and channeling the flow with a shovel. Equation 1 was used to estimate the concentration of injectate (C_1) needed for the entire reach, based on the values for discharge (Q_s) at the downstream end of the study reach (site

Table F1. Field parameters and chemical analyses of water samples collected during synoptic sampling of the Verde River headwaters, June 17-19, 2000.
[µS/cm, microsiemens per centimeter; ND, not determined; mg/L, milligrams per liter; µg/L, micrograms per liter; δ, del; *, estimated]

Lab no.	Field ID	Site description and comments	Distance[1] (ft)	Date[2]	Time	Latitude (34°)	Longitude (112°)	GPS error (ft)
C-172501	FB-00	Field blank using deionized water from USGS laboratory		06/18/2000	0000	ND	ND	ND
C-172522	DRS-1	Del Rio Spring; collected upstream from southernmost culvert along main dirt road	ND	06/19/2000	1035	49.190	26.730	+18
C-172523	LGS-1	Lower Granite Creek Spring; north of large cottonwood grove; north bank near large fallen log	-5,000	06/17/2000	1115	51.020	25.449	+9.2
C-172524	SLS-1	Stillman Lake Spring; uppermost end of lake from small disconnected spring-fed pool	-4,000	05/07/2000	0930	51.530	26.267	+78
C-172525	SLS-2	Stillman Lake Spring; small pools were dry; sampled from uppermost end of lake; lots of algae	-4,000	06/17/2000	1400	51.530	26.267	+78
C-172502	SP561	Dry channel, ground-water sample from hand-dug pit in streambed	561	06/18/2000	0920	51.822	25.830	+410
C-172503	VR635	First standing water in Verde River channel amidst thick stand of aquatic and riparian plants	635	06/18/2000	0915	51.832	25.838	+29
C-172504	VR930	Verde River sample collected from well-defined channel with measurable current	920	06/18/2000	0910	51.877	25.793	+370
C-172505	VR1200	Verde River 1,200 ft downstream from confluence; gaining reach	1,200	06/18/2000	0900	51.914	25.750	+46
C-172506	VR1300	Verde River 1,300 ft downstream from confluence; gaining reach	1,300	06/18/2000	0917	51.914	25.728	+29
C-172507	SP1350	Spring-fed pool near south bank of Verde River; 3 X 6 X 2 ft in size; low dissolved oxygen	1,430	06/18/2000	0905	51.917	25.709	+44
C-172521	SP1700	Largest flowing spring emerging from Martin Limestone, north edge of canyon near overhead power line	1,700	06/17/2000	1610	51.550	25.800	+7.8
C-172508	VR2000	Verde River 2,000 ft downstream from confluence; below inflow from largest spring; gaining reach	2,000	06/18/2000	0905	51.913	25.623	+380
C-172509	SP2300	Large spring-fed pond on south edge of canyon at base of canyon wall; about 70 X 30 X 5 ft in size	2,300	06/17/2000	1535	51.915	25.589	+45
C-172510	SP2625	Flowing spring on north edge of stream channel, emerging from aquatic plants	2,625	06/18/2000	1050	51.925	25.528	+34
C-172511	SP2650	Flowing spring on south edge of stream channel	2,650	06/18/2000	1100	51.916	25.536	+56
C-172512	SP2915	Flowing spring on north edge of stream channel, emerging from aquatic plants	2,915	06/18/2000	1110	51.926	25.489	+55
C-172513	VR3000	Verde River 3,000 ft downstream from confluence	3,000	06/18/2000	0900	51.946	25.487	+29
C-172514	VR4000	Verde River, 4,000 ft downstream from confluence; near mouth of “Greenbie Gulch”	4,000	06/18/2000	1000	51.985	25.365	+27
C-172515	SP4610	South side of channel, small seep at upstream end of small shallow inlet; sampled with dipper	4,610	06/18/2000	1030	52.015	25.283	+33
C-172516	VR5000	Verde River 5,000 ft downstream from confluence	5,000	06/18/2000	0950	52.025	25.235	+31
C-172517	VR5000	Duplicate sample	5,000	06/18/2000	0950	52.025	25.235	+31
C-172518	VR6000	Verde River 6,000 ft downstream from confluence	6,000	06/18/2000	0940	52.033	25.097	+31
C-172519	VR7800	Verde River 7,000 ft downstream from confluence	8,000	06/18/2000	0930	52.091	24.875	+42
C-172520	VR13460	Verde River at Stewart Ranch 13,460 ft downstream from confluence, near gate in fence	13,660	06/18/2000	0900	52.080	24.019	+36
C-220225	MDN-1	Unnamed spring on north bank of Verde River near mouth of Muldoon Canyon, river mile 8	ND	05/16/2003	0200	86.710	35.450	+40

Table F1. Field parameters and chemical analyses of water samples collected during synoptic sampling of the Verde River headwaters, June 17-19, 2000. (Continued)

[µS/cm, microsiemens per centimeter; ND, not determined; mg/L, milligrams per liter; µg/L, micrograms per liter; δ, del; *, estimated]

Lab no.	Field ID	Dissolved oxygen (mg/L)	pH	SC (µS/cm)	T	HCO_3 (mg/L)	Alkalinity (Lab)	Alkalinity (Field)	Discharge[3] (ft^3/s)	Cl[4] (mg/L)	Ca (mg/L)	Mg (mg/L)	Na[4] (mg/L)	F (mg/L)	NO^3 (mg/L)
C-172501	FB-00	--	--	--	--	--	--	--		<1.2	<0.1	<0.1	<0.1	<0.08	<0.35
C-172522	DRS-1	5.55	7.55	345	18.5	151	123	124	ND	18.5	46	21	21	0.5	6.2
C-172523	LGS-1	2.48	7.30	458	18.9	226	253	185	ND	20.8	48	22	20	0.5	4.6
C-172524	SLS-1	0.83	6.84	546	15.2	293	245	240	ND	20.7	56	24	21	0.4	1.3
C-172525	SLS-2	5.87	8.13	454	28.0	251	157	206	ND	14.5	87	40	9.2	0.4	<0.35
C-172502	SP561	0.88	6.00	570	22.2	305	259	250	0.05*	**31.9**	64	25	**29**	0.4	0.6
C-172503	VR635	0.54	5.99	523	12.1	305	244	250	0.5*	20.4	52	22	21	0.4	<0.35
C-172504	VR930	4.50	6.90	451	17.0	238	197	190	1.0	**76.4**	46	20	**62**	0.4	2.9
C-172505	VR1200	3.06	7.17	439	19.5	229	190	187	2.3	**45.0**	40	18	**37**	0.4	4
C-172506	VR1300	10.13	7.48	439	19.7	244	193	200	2.7	**41.5**	40	18	**36**	0.4	4.1
C-172507	SP1350	0.97	7.40	598	20.4	354	284	290	ND	22.5	62	26	37	0.4	<0.35
C-172521	SP1700	6.87	7.41	552	19.8	285	--	234	0.5*	23.9	30	16	17	0.5	4.1
C-172508	VR2000	8.44	7.16	484	20.9	256	212	210	5.4	**29.7**	42	20	**37**	0.5	4.7
C-172509	SP2300	2.23	7.08	557	25.0	293	--	240	ND	20.0	43	23	46	0.5	1.3
C-172510	SP2625	5.72	7.06	579	21.1	305	240	250	ND	19.3	45	22	44	0.5	5.6
C-172511	SP2650	6.25	7.30	584	20.0	329	260	270	ND	19.4	42	21	44	0.5	5.9
C-172512	SP2915	0.57	6.88	663	24.7	354	293	290	ND	22.8	46	23	47	0.5	<0.35
C-172513	VR3000	5.39	7.00	553	21.1	281	198	230	13.8	**23.3**	43	21	**40**	0.5	5
C-172514	VR4000	7.83	7.06	596	21.7	334	260	270	13.7	**23.4**	44	22	**48**	0.5	5
C-172515	SP4610	1.16	7.33	642	21.4	354	303	290	ND	22.5	53	26	60	0.5	2.4
C-172516	VR5000	7.16	7.04	634	22.2	390	283	320	19.7	**23.9**	49	24	**57**	0.5	5
C-172517	VR5000	--	--	--	--	--	--	--	19.3	**24.0**	49	24	**58**	0.5	5
C-172518	VR6000	7.44	7.53	634	22.4	329	263	270	21.3	**23.7**	51	26	**61**	0.6	4.6
C-172519	VR7800	9.32	7.85	637	24.5	354	286	290	18.6	**24.1**	48	24	**57**	0.5	4.4
C-172520	VR13460	7.81	8.14	637	25.1	348	256	285	19.5	**23.8**	44	22	**59**	0.5	4.2
C-220225	MDN-1	4.40	6.80	704	18.2	330	--	270	<1*	**23.0**	0.5	25	**57**	0.5	<0.08

Table F1. Field parameters and chemical analyses of water samples collected during synoptic sampling of the Verde River headwaters, June 17-19, 2000. (Continued)

[µS/cm, microsiemens per centimeter; ND, not determined; mg/L, milligrams per liter; µg/L, micrograms per liter; δ, del; *, estimated]

Lab no.	Field ID	SO_4 (mg/L)	Si (mg/L)	K (mg/L)	Al (µg/L)	As (µg/L)	B (µg/L)	Ba (µg/L)	Fe (µg/L)	Li (µg/L)	Mn (µg/L)	Sr (µg/L)	V (µg/L)	$\delta^{18}O$ per mil	δD per mil
C-172501	FB-00	<1.6	<0.1	<0.1	<10	<100	14	<1	<50	<10	<10	<1	<10	--	--
C-172522	DRS-1	14	16	2.4	0.83	11	41	8.7	15	<10	14	500	15	-10.1	-72
C-172523	LGS-1	13	20	2.9	7.8	16	81	31	22	12	28	620	11	-9.7	-70
C-172524	SLS-1	15	18	3.8	8.2	12	80	170	61	17	260	540	<10	-8.7	-66
C-172525	SLS-2	13	16	2.5	3.6	6.7	70	92	44	15	1100	560	<10	-8.3	-65
C-172502	SP561	21	17	4.1	<10	<100	80	160	<50	17	780	650	17	-9.5	-69
C-172503	VR635	11	16	2.7	<10	<100	74	81	<50	<10	480	540	<10	--	--
C-172504	VR930	12	18	3	<10	<100	77	40	<50	15	12	480	12	-9.8	-71
C-172505	VR1200	12	18	2.8	<10	<100	82	32	<50	17	<10	410	12	-10.1	-72
C-172506	VR1300	12	19	2.8	<10	<100	85	32	<50	18	<10	410	12	-10.1	-72
C-172507	SP1350	5.8	30	5.3	1.6	13	150	95	82	27	320	560	<10	-9.2	-69
C-172521	SP1700	15	20	3	16	19	200	45	35	36	<10	390	13	-10.3	-75
C-172508	VR2000	13	20	2.9	<10	<100	120	38	<50	24	<10	410	13	-10.2	-73
C-172509	SP2300	14	13	4	4.8	17	200	49	30	39	18	380	<10	--	--
C-172510	SP2625	14	20	3	6.1	20	210	47	28	39	<10	380	13	-10.4	-75
C-172511	SP2650	14	19	2.8	7.4	21	200	45	28	37	<10	360	12	-10.4	-75
C-172512	SP2915	13	20	6.2	2.4	29	200	57	65	39	540	400	<10	-10.3	-74
C-172513	VR3000	13	20	2.9	<10	<100	170	41	<50	31	<10	400	13	-10.3	-74
C-172514	VR4000	14	19	3.1	<10	<100	210	47	<50	39	<10	380	12	-10.3	-74
C-172515	SP4610	16	21	3.3	8.6	29	270	60	34	49	11	440	13	-10.4	-75
C-172516	VR5000	15	20	3.2	<10	<100	250	52	<50	47	<10	390	12	-10.3	-75
C-172517	VR5000	15	20	3.3	<10	<100	240	53	<50	47	<10	410	13	--	--
C-172518	VR6000	15	21	3.4	<10	<100	260	55	<50	49	<10	430	13	-10.4	-75
C-172519	VR7800	15	19	3.2	<10	<100	240	52	<50	47	<10	390	12	-10.5	-74
C-172520	VR13460	15	20	3.2	<10	<100	250	55	<50	48	<10	420	12	-10.5	-75
C-220225	MDN-1	23	19	2.6	0.71	26	260	110	40	41	12	380	0.8	-10.0	-74.0

[1]Distance is the distance in feet downstream from the confluence with Granite Creek as defined by the center of the natural dam at Stillman Lake.

[2]Field parameters collected during field reconnaissance June 14-17, 2000.

[3]Calculated using chloride concentration, except where indicated by asterisks.

[4]Bold value indicates stream sample was downstream from the injection site (non-background).

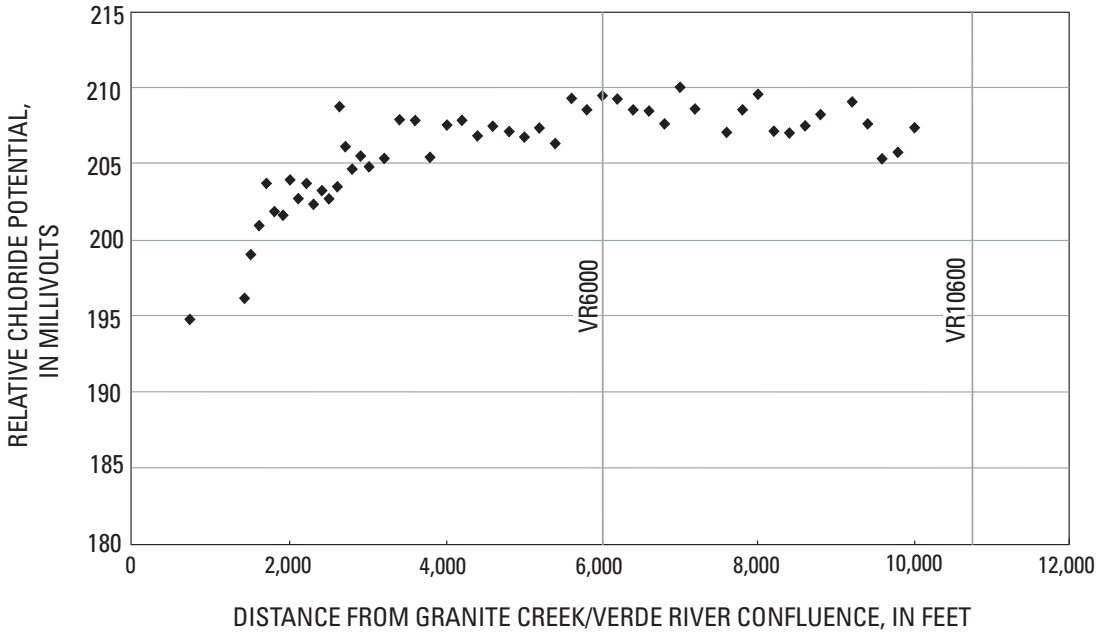

Figure F6. Graph showing relative chloride potential with distance along the tracer reach, which is inversely related to chloride concentration. In order to monitor the distribution of the chloride tracer, measurements of relative chloride potential were made using a selective-ion probe over a three-day timeframe. Variations in chloride distribution are related to the degree of mixing and to diurnal variations in discharge.

VR13640 at Stewart Ranch on June 13, 2000) and predetermined concentrations of chloride in the upper Verde River (C_A and C_B) from an earlier seepage study (Boner and others, 1991). Current-meter measurements were made at the beginning and end of the study reach (sites VR930 and VR13460) and at two sites in lower Granite Creek with good channel control that were outside of the tracer reach. Discharge from Stillman Lake could not be determined using a current meter because the velocity of the lake current was too slow.

Tracer-dilution Equipment

To prepare the tracer solution, granular NaCl was mixed with streamwater to saturation level several hours before the injection. A 500-gallon nalgene tank and thirty-five 50-lb bags of stock salt were shuttled to the injection site using an all-terrain vehicle. Small batches of injectate solution were premixed in a 55-gallon reservoir with a canoe paddle until the solution reached saturation and then transferred as needed to keep the larger reservoir tank filled. An excess of undissolved NaCl always was present in the bottom of the larger reservoir to maintain a state of saturation and the tank was periodically stirred. Injectate samples were collected throughout the tracer study to verify that the concentration of the solution remained fairly constant.

The injection apparatus consisted of a piston-core pump driven by an electric motor that was powered by a deep-cell marine battery. Tracer solution (NaCl) was pumped from the large reservoir through plastic tubing to a prepump filter capsule and then through the pump to the stream. Injection of the tracer solution at site VR900 started at 1800 hours on June 15 and continued until 1200 on June 18. A bubble meter was used to monitor the rate of injection to ensure that the pump was working properly and that the flux of tracer was steady. In addition, the injection rate was measured periodically with a volumetric flask and stopwatch to make sure that it remained constant.

Automatic Samplers

Hourly stream samples were collected by three ISCO®™ automatic samplers (sites T1, T2, and T3 in fig. F1) to monitor the concentration of the tracer solution in streamflow (fig. F7). The hourly samples were analyzed later for chloride concentrations at a USGS laboratory in Denver, Colorado (see discussion of analytical methods below) to determine tracer arrival and recovery times and to verify that the salt tracer was close to steady-state conditions during the synoptic sampling. Steady-state tracer conditions are required to accurately measure discharge.

Sampler T1 was deployed near the beginning of the reach below the injection point at site VR900 and T2 was deployed at the end of the study reach at Stewart Ranch (site VR13640). The intake for T3 at site VR1300 was inadvertently located at a

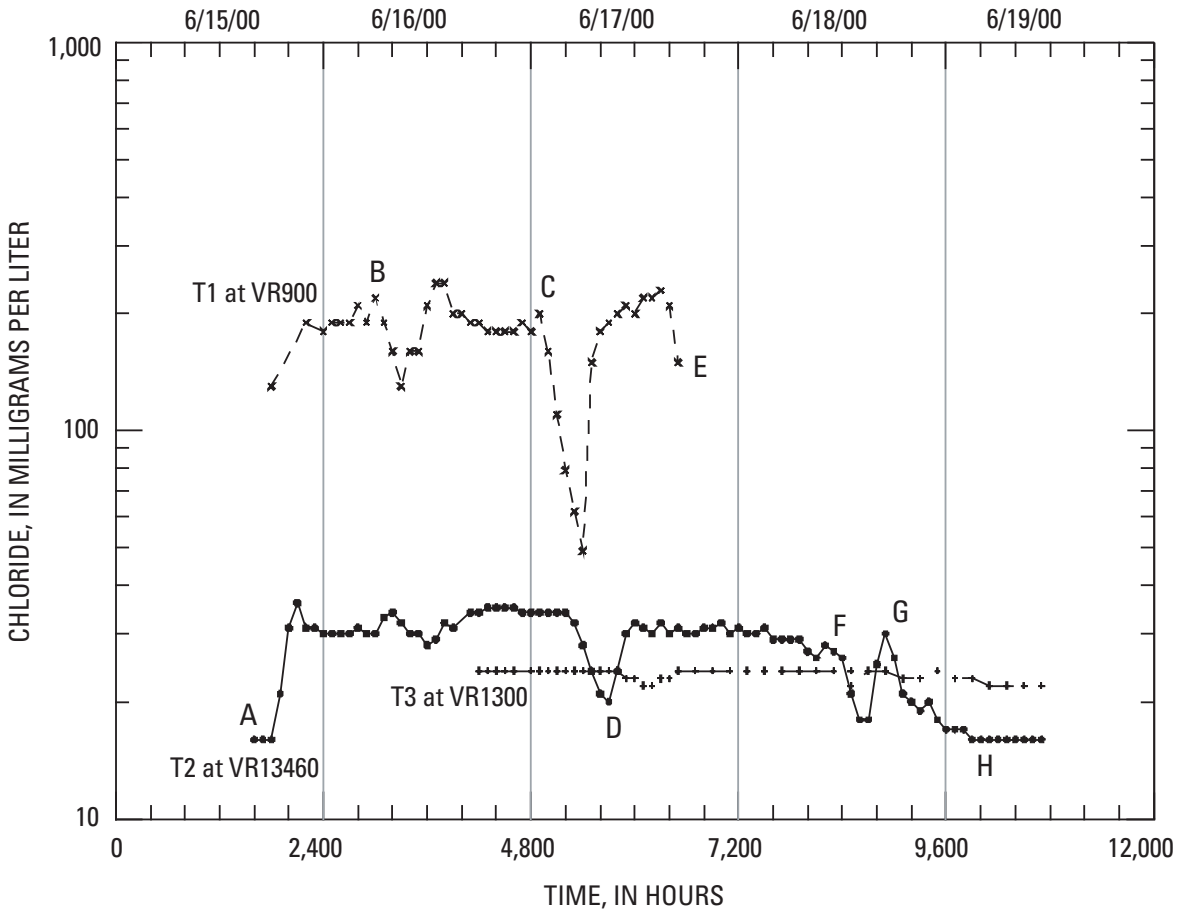

EXPLANATION

A, Tracer injection begins at 1800 hours
B, Pump battery dies before daybreak
C, Pump battery disconnected by cow at about 1300 hours
D, Lag time from VR900 to VR13460 about 2-3 hours (estimated)
E, ISCO sampler at VR900 discontinued to conserve sample bottles
F, Synoptic sampling from 0900 to 1000 hours on 6/18/2000. Tracer injection ends at 1000 hours
G, Slug of remaining tracer solution from emptied tank
H, Background conditions resumed

Figure F7. Field notes and graph explaining variations in tracer concentrations versus time at each of three automatic samplers. Samples were collected hourly. Locations of automatic samplers are shown on figure F1.

location where ground water was discharging to the bottom of the stream; consequently, the sampler collected unmixed inflow from upper Verde River springs instead of fully mixed streamflow. This was not realized until much later when the analytical results became available. Apparently, the intake tubing rested on the streambed in a gaining area that displaced the tracer solution with no significant mixing. The T3 results were unintended but do show that concentrations of chloride in spring inflow did not vary substantially with time. The background concentration of chloride in ground water discharging near upper Verde River springs was 23.5+0.7 mg/L (n = 45) and varied by 3 percent between June 16 and 19, 2000, which is similar in magnitude to the reported analytical accuracy (discussed below).

An injection rate of 9.3 milliliters per second was maintained throughout the study, with the exception of two accidental power-supply interruptions (fig. F7). The first interruption occurred when the battery ran down on June 16 at 0400, shortly before dawn. A second interruption occurred on June 17 at about 0100, when a cow dislodged the wire cables between the pump and the battery. In each instance, the pump ceased for several hours, but the tracer resumed steady-state conditions quickly because of the rapid travel time through

the reach. Thus, neither interruption appears to have had a lingering effect on tracer concentrations during the synoptic sampling on the morning of June 18. At the time of the synoptic sampling, the injection of tracer had been continuous for more than 24 hours without interruptions. The rate of injection appears to have been declining gradually through the previous night, which is attributed to the pump batteries gradually losing their charge. Given the rapid travel time through the reach, however, the distribution of tracer appears to have been close to steady-state conditions and should have been well mixed in the slower moving parts of the channel.

As mentioned earlier, because chloride determinations by selective-ion probe are less accurate than by ion chromatography, the probe method was used primarily for reconnaissance to show the arrival of tracer and that the tracer solution was well mixed throughout the stream reach (fig. F6). Tracer concentrations at site VR13460 could only be verified much later when the analytical results for the T2 samples became available. Although initial velocity measurements indicated that the tracer solution could traverse the 2.5-mi reach in several hours, there was concern that the density of aquatic vegetation would prevent the tracer from evenly mixing through the water column. Most tracer-dilution studies have been conducted in high-gradient mountain streams (Zellweger, 1996; Kimball, 1997; Kimball and others, 1999; Walton-Day and others, 1999; Wirt and others, 2000; 2001) so the utility of the technique in a relatively low-gradient canyon setting having thick riparian vegetation was largely untested. How well the tracer would mix through the stream, given the dense aquatic vegetation at the upper end of the reach and the presence of a large-volume, slow-moving reach impounded by a beaver dam near site VR7800, was unknown. To compensate for these conditions, the injection of tracer was extended for 60 hours or as long as reasonably possible given staffing constraints. In hindsight (and without the power interruptions), 6 hours probably would have been adequate to reach and maintain steady-state conditions. The end result was that tracer conditions were fairly steady for 24 hours leading up to the synoptic study and are thought to have been well mixed at all sites (except possibly synoptic site VR7800, in deep, slow water behind a beaver dam).

Synoptic Sampling

Synoptic samples were collected by three teams, between 0900 and 1000 hours on June 18, during what probably was close to the peak discharge of the diurnal cycle. The analytical results are reported in table F1. The injection pump was shut off as soon as the synoptic sampling was completed. Chloride concentrations at site VR13460 returned to background levels after approximately 2–3 hours (fig. F7).

Water-chemistry samples were collected at selected springs and all synoptic sites using standard USGS methods comparable to Wilde and others (1999). The width of the Verde River increased from about 3 to 20 ft over the reach. A representative sample was collected at each site by immersing an open, hand-held 1- or 2-L plastic bottle in the centroid of flow or at multiple verticals as described by Shelton (1994).

Sample Processing, Analytical Methods, and Analytical Uncertainty

Filtering and processing were done in the field, using standard USGS equipment and protocols (Horowitz and others, 1994). All samples were processed within a 12-hour period on the same day they were collected. Water samples were filtered using a 0.45-µm syringe-mounted capsule filter. Sample splits for major-ion analysis were preserved by adding ultrapure nitric acid to a pH of < 2. Major elements were determined at a USGS laboratory in Denver, Colorado, by inductively coupled plasma-atomic emission spectrometry (ICP-AES; Briggs and Fey, 1996). Concentrations of the chloride, nitrate, fluoride, and sulfate were determined by ion chromatography from filtered, unacidified samples (d'Angelo and Ficklin, 1996). The quality of the laboratory analyses was assessed through analysis of laboratory blanks, sample duplicates, and USGS standard reference water samples (Long and Farrar, 1995). Field parameters and analytical data for dissolved cations and anions are listed in table F1. Stable isotope analyses were conducted by the Laboratory of Isotope Geochemistry at the University of Arizona in Tucson, Arizona.

The accuracy of chloride analyses in synoptic samples by ion chromatography was considered critical and was determined using USGS standard reference water samples (Long and Farrar, 1995). A low-range standard of 25.8 mg/L was run 4 times and had a standard deviation of ± 1.4 mg/L. A high-range standard of 65 mg/L was run twice with a standard deviation of ± 2.1 mg/L. Thus, the analytical uncertainty for the discharge measurements using the tracer-dilution technique is about ± 5 percent for low-range chloride concentrations and ± 3 percent for high-range chloride concentrations.

Results

Calculated Base Flow

A total base flow of 19.5±1.0 ft^3/s was calculated for the end of the tracer reach at Stewart Ranch (during near-peak conditions), compared with a peak daily flow of 21.2±1.0 ft^3/s at the Paulden gauge. By subtraction, approximately 7 percent of base flow at the Paulden gauge was contributed downstream from the tracer reach. Seepage has been observed on both banks of the Verde River downstream from the mouth of Muldoon Canyon (river mi 8), which is thought to account for most of the missing inflow. The Little Chino basin-fill aquifer delivered 13.8±0.7 percent of the total base flow (2.7±0.08 ft^3/s) upstream from site VR1200. This Little Chino fraction is substantially higher than the 8.4 percent contribution from the Little Chino basin-fill aquifer predicted

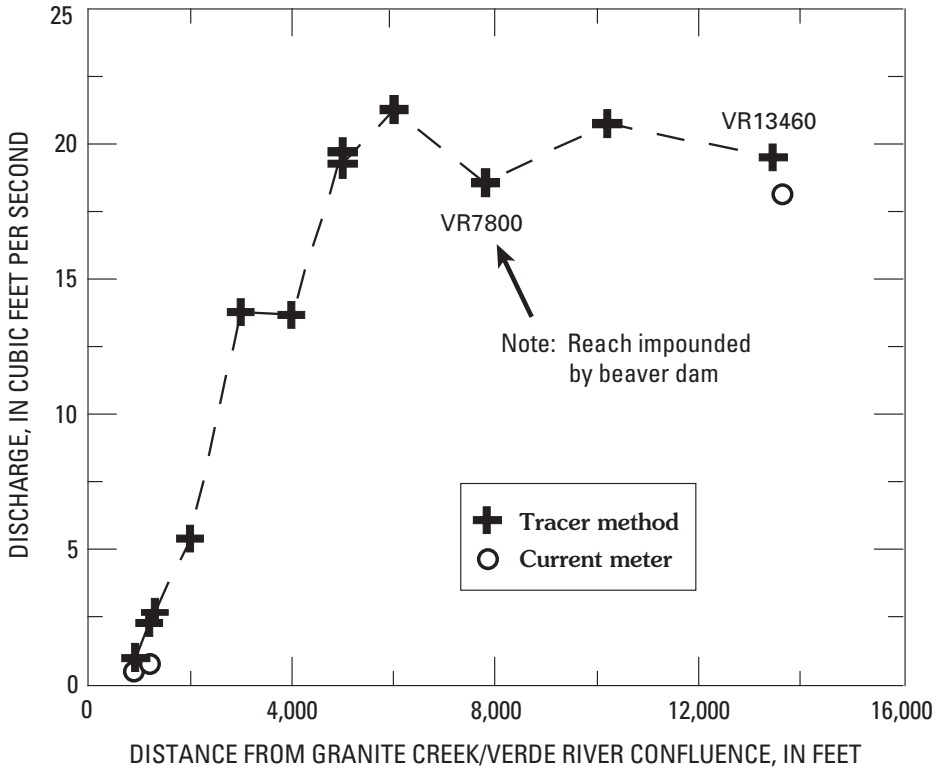

Figure F8. Graph showing discharge calculated from tracer-dilution study versus distance downstream on June 18, 2000. Synoptic sampling occurred between 0900 and 1000 hours. Current-meter measurement at VR13460 was made at 1343 hours and rated as good (± 5%).

by the conceptual 1990s water-budget model presented in the introductory chapter (Wirt, Chapter A, this volume, fig. A16 and table A4) and is thought to provide a more accurate baseline of current conditions.

Accuracy of Discharge Calculations

Discharge was calculated from analytically determined concentrations of chloride at each synoptic stream site using equations 1.0 and 2.0 (figs. F5 and F8). Discharge values are most accurate in the first mile of the study reach where the tracer concentrations greatly exceed the natural chloride concentrations (fig. F8). In the beginning of the tracer reach, the contrast between tracer concentrations and background concentrations of chloride is large (table F1) and the method uncertainty approaches the uncertainty of the high-range analytical method for chloride, which was about 5 percent. Between sites VR3000 and VR13460, instream concentrations of chloride tracer approached the background concentrations of chloride measured from springs, although the low-range analytical uncertainty decreased to about 3 percent.

Tracer concentrations downstream from site VR3000 varied from 23.3 to 24.1 mg/L. In comparison, background chloride concentrations determined for upper Verde River springs varied between 19.3 to 23.9 mg/L (table F1), with an average background value of 19.6 mg/L (n = 7 springs). It was not possible to flowweight the background chloride levels from different spring inflows; however, the mean value was 15 percent less than the chloride range measured for the stream and is thought to accurately represent background conditions. Near site VR7800, slow-moving backwater behind a beaver dam may have caused incomplete mixing along the marshy edges of the wide, deep reach.

Potential tracer method uncertainty is the sum of (a) analytical uncertainty, (b) uncertainty of the range of variation in background chloride levels, (c) amount of change in stage attributed to diurnal changes, and (d) uncertainty of the degree of mixing of the tracer in the stream. The amount of analytical uncertainty is known, and an effort was made in the design of the study to minimize the effects of the other unknown factors by measuring background chloride in springs, by continuing the injection phase as long as feasible to establish steady-state conditions, and by restricting the synoptic sampling to 1 hour.

The analytically determined discharge is within 10 percent of that determined by current-meter measurements (fig. F8). By using the tracer-dilution method, the discharge calculated at the lower end of the tracer reach was 19.5±1.0 ft^3/s at 0900 hours on June 18, 2000, at site VR13460. In comparison, a discharge of 17.7±1.0 ft^3/s was measured using a current

meter at 1343 hours, almost 5 hours later on the same day. In addition, 17.4±1.4 ft^3/s was measured using a current meter at 1110 hours on June 13, 2000. Given that the current-meter measurements were made 2 to 5 hours later on the falling limb of the diurnal cycle, the measurements are in reasonable agreement, although the tracer measurement is considered more representative of the peak daily discharge. An additional factor that may explain part of the disparity is that current-meter measurements tend to underestimate the amount of base flow by neglecting the fraction that occurs as hyporheic flow. Thus, the 2.1 ft^3/s difference between the two methods is attributed to (1) falling stage resulting from diurnal variations, (2) a fraction of base flow occurring as hyporheic flow, (3) measurement uncertainties for both methods, or (4) a combination of these three factors.

Changes in Water Chemistry with Distance Downstream

Spatial changes in stream chemistry result from a variety of simple processes. Physical changes in temperature, pH, and the concentration of dissolved gases occurred as ground water discharging to the stream equilibrated with the atmosphere. Water chemistry also changed in response to mixing between different sources of water and from geochemical processes such as leaching or dissolution of rock-forming minerals. This section presents downstream variation in field parameters and selected cations, anions, trace elements, and in the stable isotope composition of oxygen and hydrogen with distance along the study reach. Water-chemistry data are presented in figures F9–F14 and reported in table F1.

Field Parameters

Specific conductance, water temperature, and pH were measured as part of the field reconnaissance of lower Granite Creek, Stillman Lake, and the upper Verde River. Reconnaissance field data were collected at many sites in addition to the synoptic sites (presented in table F1 and subsequent figures). Reconnaissance data in figure F9 were graphed in the field to select the synoptic sampling sites.

Specific conductance is the ability of a substance to conduct an electrical current, which in dilute solutions is directly related to the concentration of dissolved salts (Hem, 1992). Specific conductance increased along the length of lower Granite Creek from about 460 microSiemens per centimeter (μS/cm) at Lower Granite Spring (site LGS-1) to about 550 μS/cm near its mouth, as indicated by the dashed best-fit regression line (fig. F9A). The increase in dissolved salts is most likely caused by water-rock interaction but also could be caused by evaporation of surface water. The increasing trend extended beyond the mouth of Granite Creek toward two small seeps near the beginning of the first seepage in the upper Verde River channel (sites SP561 and SP1350, with 570 and 598 μS/cm, respectively). Based on the field data, the two seeps are interpreted to represent shallow ground water derived from the Granite Creek area, as indicated by their orange "X" symbols in figure F9.

A decreasing trend in conductance was observed over the length of Stillman Lake. Specific conductance ranged from about 550 μS/cm at the upstream end of the lake to 360 μS/cm at the downstream end. This is surprising in that evaporation or dissolution of rock-forming minerals would be expected to produce an increase rather than a decrease in specific conductance along the flow gradient. The simplest explanation for this occurrence is a high-conductance inflow discharging to the upstream end of the lake and a low-conductance inflow discharging to the downstream end of the lake.

Specific conductance of the initial flow in the upper Verde River at site VR635 (523 μS/cm) was more similar to that at the mouth of Granite Creek (550 μS/cm) than to that at the lower end of Stillman Lake (360 μS/cm). Conductance initially decreased between sites VR635 and VR900 from 523 to 410 μS/cm. The decrease appears to be caused by mixing between ground-water inflows from Granite Creek and Stillman Lake. At site VR930, this trend was abruptly reversed, and specific conductance (and discharge) increased, owing to a third source of ground-water inflow from upper Verde River springs. Specific conductance for the upper Verde River springs network ranged between 550 and 642 μS/cm. Downstream from site VR5000, specific conductance reached a plateau indicating no new inflows with distinct geochemical characteristics and what probably is the end of the gaining reach.

In ground-water studies, similar water temperatures can be an indication that ground waters have undergone a similar cooling regime, which provides one piece of evidence that the sources could be similar. Temperature is not a conclusive line of evidence because water temperatures can change in response to sunlight, air temperature, and other variables. Not surprisingly, the highest water temperatures were measured near the edges of Stillman Lake, where water was shallow, slow moving, and in direct sunlight (fig. F9B). The lowest temperatures of about 15 degrees Celsius (°C) were measured from the bottom of a small pool in lower Granite Creek (site GC1500) and a spring inflow at the upstream end of Stillman Lake (site SLS-1). The similarity of the water temperatures near two widely spaced inflows in Stillman Lake and lower Granite Creek (both having specific conductance of about 550 μS/cm) suggests a similar ground-water origin, although not at all conclusively. Similarities in the composition of hydrogen and oxygen stable isotopes and strontium concentrations presented in Chapter E (Wirt and DeWitt, this volume) and later in this chapter provide more compelling evidence that the common origin of ground-water discharge to lower Granite Creek and Stillman Lake is the Little Chino basin-fill aquifer. In general, the water temperature of Granite Creek increased with distance downstream from site GC1500 and also increased in a nonlinear fashion from the upstream to the downstream end of Stillman Lake.

Temperature variations suggest at least two ground-water inflows near the beginning of the upper Verde River.

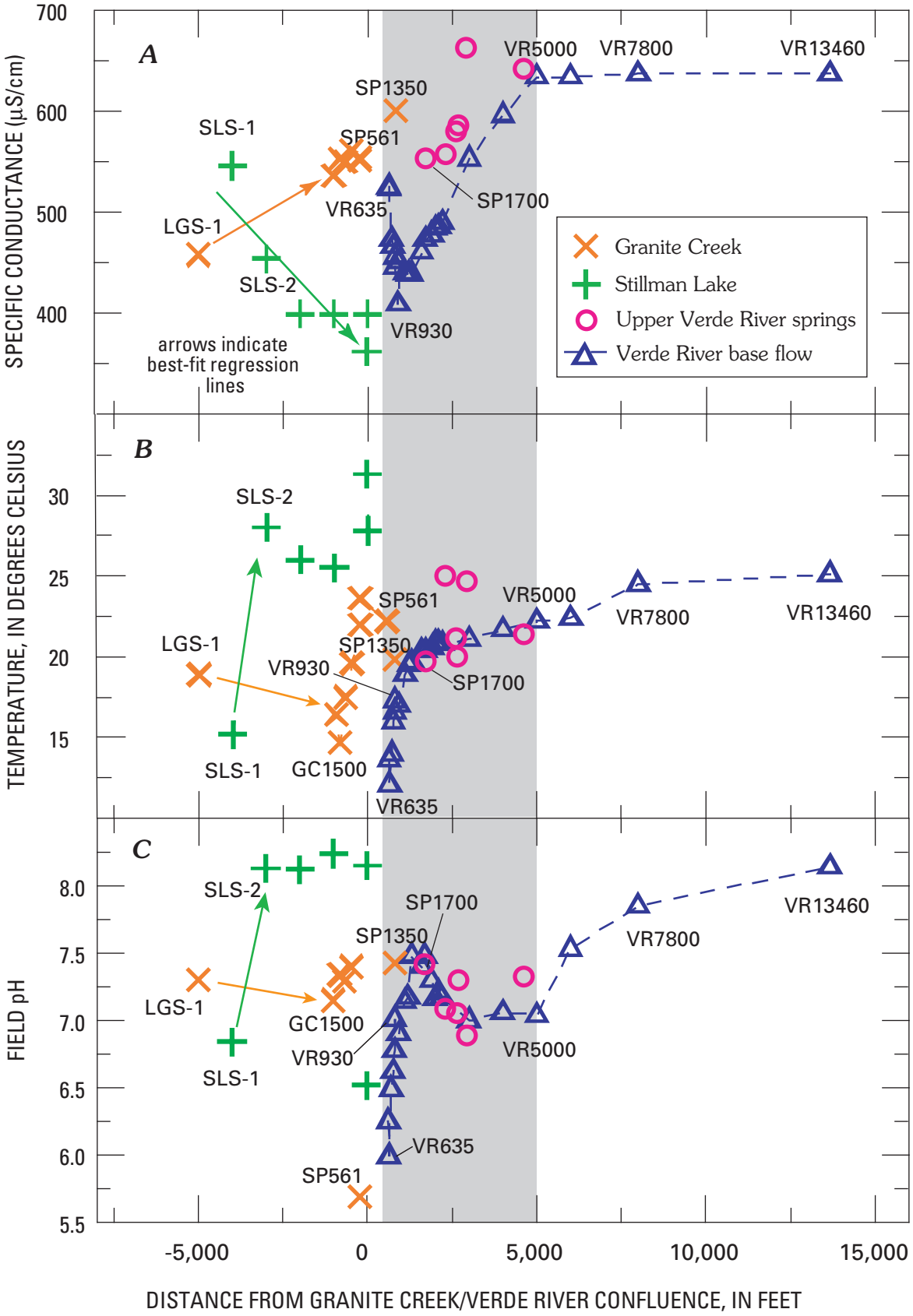

Figure F9. Graphs showing changes in (*A*) specific conductance, (*B*) water temperature, and (*C*) pH versus distance from Granite Creek/Verde River confluence. Shaded area indicates extent of gaining reach.

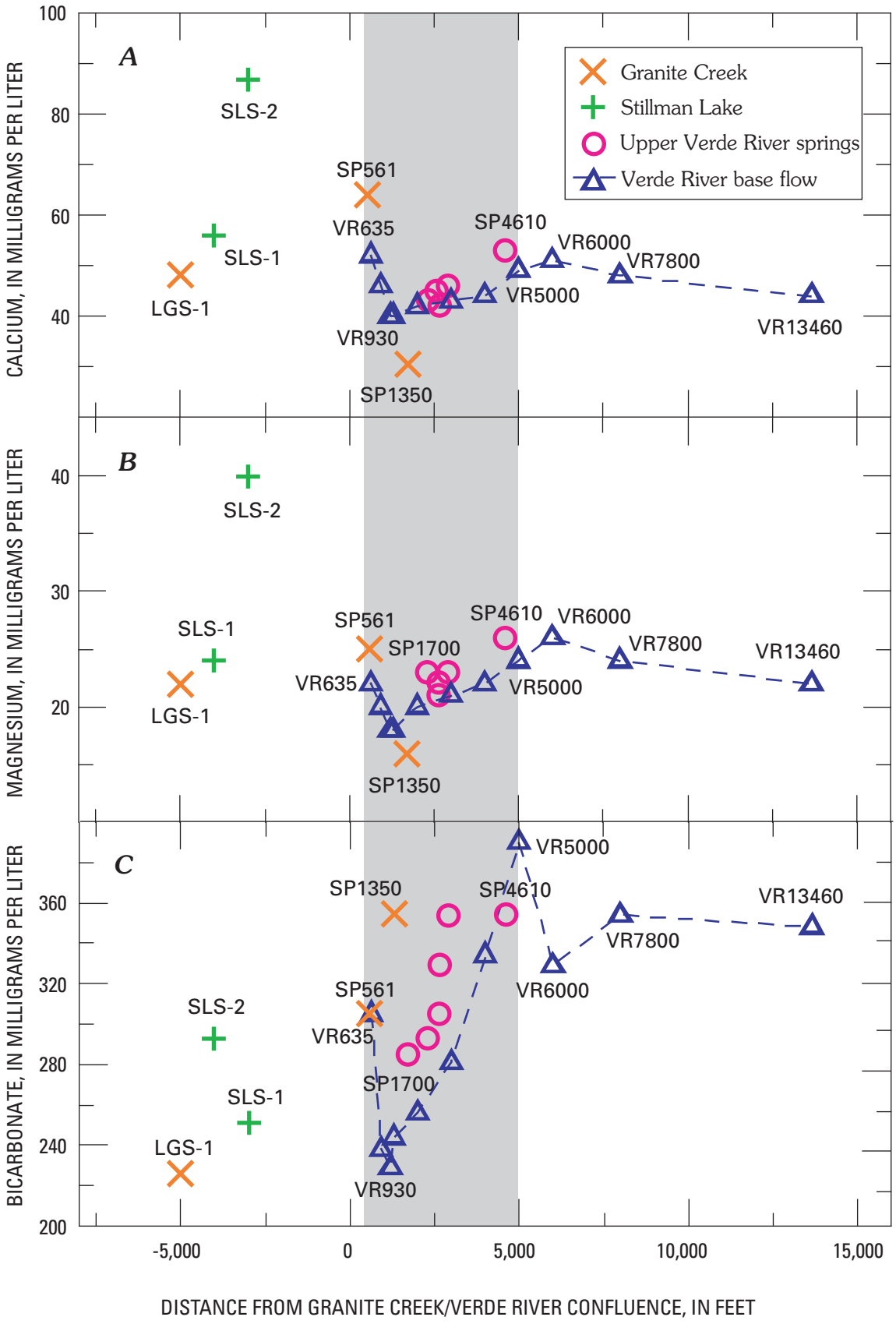

Figure F10. Graphs showing changes in (*A*) calcium, (*B*) magnesium, and (*C*) bicarbonate versus distance from Granite Creek/Verde River confluence. Shaded area indicates extent of gaining reach.

The lowest water temperature for the entire study of 12.1°C was at site VR635, in comparison to air temperatures measured in excess of 35°C during the day. The source of this colder inflow is attributed to a Little Chino source. In contrast, the minimum temperature measured for upper Verde River springs was 19.8 °C, with a mean water temperature of 21.7±2.2°C (n = 7) or nearly 10 degrees higher than at VR635. Downstream from the gaining reach, the streamflow temperature increased to 25.1°C at site VR13460, as base flow was warmed by air and sunlight.

Variations in pH in the Verde River correlated with the degree of contact that water has had with the atmosphere (fig. F9C). All pH values less than 7.0 were measured from sites where ground-water inflow was evident. Most of these sites were in the immediate vicinity of the confluence of Granite Creek and the Verde River. In Stillman Lake, the lowest pH value of 6.5 (site SLS-3 at the downstream end), which also had the lowest specific conductance within the study area (360 µS/cm), indicating unmixed inflow. In lower Granite Creek, a similar pH of 6.7 was measured near the mouth. The lowest pH of 6.0 for the entire study area was measured downstream at site VR635 in the Verde River, which also had the lowest measured temperature. All three sites had a Little Chino source and were in relatively close spatial proximity, although disconnected by a dry stream segment. In contrast, the highest pH measurements exceeded 8.0 along the edges of Stillman Lake and also at site VR13460. These were sites where no ground-water inflows were occurring and there was ample contact with the atmosphere allowing degassing of carbon dioxide.

Changes in pH (or hydrogen-ion activity) are related to temperature, alkalinity, and interrelated chemical reactions, particularly the degassing of CO_2 and the dissolution of calcite (Hem, 1992). The pH is a useful index of geochemical reactions in which the water participates. For example, dissolution of calcite ($CaCO_3$) results in an increase in HCO_3^- and a corresponding increase in pH. A decrease in dissolved CO_2, which is produced from biological activity in the unsaturated zone, also will cause pH to increase. Because the concentration of CO_2 in the soil zone is often as high as 5 percent and the atmospheric concentration is about 0.03 percent, dissolved CO_2 is rapidly lost as shallow ground water seeps into a stream bed (Bullen and Kendall, 1998).

The pH increased from 6.0 to 8.1 in a non-linear pattern between sites VR635 and VR13460 (fig. F9C). An initial increase in pH from 6.0 to 7.5 between sites VR635 and VR1700 is attributed to rapid degassing of CO_2 from Granite Creek and Stillman Lake inflow. In the vicinity of upper Verde River springs, the stream pH decreased slightly to less than 7.2. Many of the spring inflows had dissolved oxygen values of less than about 5 mg/L (table F1), an indication that the ground water had not yet equilibrated with the atmosphere. The concentration of dissolved oxygen is a function of temperature and pressure and to a lesser degree, the concentration of other solutes (Hem, 1992). At 30°C, the saturation point of dissolved oxygen in fresh water is 7.54 mg/L (Hem, 1992). Within 1.5 mi downstream from the gaining reach (site VR 13460), ground-water inflow had equilibrated with the atmosphere, as indicated by saturated conditions for dissolved oxygen (7.9 mg/L at site VR7800, table F1). The increase in the dissolved oxygen of the streamflow presumably was accompanied by degassing of CO_2. Downstream from the gaining reach (sites VR5000 to VR13460), the pH of the streamflow further increased to 8.1, which also correlates with increasing water temperature and a lack of ground-water inflows. An additional possibility that will be tested by geochemical modeling later in this chapter, is that dissolution of carbonate minerals in the Martin Limestone could also contribute, in part, to the increase in pH through this reach.

Major Elements

Ground waters in the upper Verde River headwaters area are predominantly calcium-bicarbonate waters with variable proportions of magnesium and sodium. Calcium (Ca^{+2}) and bicarbonate (HCO_3^-) typically are governed by the availability of carbonate minerals and by solution- and gas-phase equilibria involving carbon dioxide (Hem, 1992). Where dolomite is present, the behavior of dissolved magnesium (Mg^{+2}) generally is related to carbonate reactions, although its behavior is more complicated than that of Ca^{+2}.

In fig. F10, concentrations of Ca^{+2}, Mg^{+2}, and HCO_3^- are plotted versus the distance above and below the Granite Creek/Verde River confluence. In the short reach between sites VR635 and VR930, Ca^{+2} and Mg^{+2} concentrations decreased, presumably as a result of mixing between Granite Creek and Stillman Lake inflows. Bicarbonate also decreased between sites VR635 to VR930, presumably from degassing of CO_2 and a correponding increase in pH, as well as from mixing. In the middle segment between sitesVR1300 and VR5000, Ca^{+2}, Mg^{+2}, and HCO_3^- increased due to mixing with inflow from upper Verde River springs. Downstream from site VR6000, dissolved Ca^{+2} and Mg^{+2} concentrations decreased slightly, perhaps in response to a concurrent increase in pH (fig. F9). The increasing pH is largely attributed to degassing of CO_2 from emerging ground water. Bicarbonate sharply decreased from VR5000 to VR6000 in the absence of spring inflows, then stabilized between sites VR7800 and VR13460.

Concentrations of major cations generally are related to geochemical processes involving the distribution of minerals and the length of the ground-water flowpath. Mineral saturation indices (SI, where SI = log IAP/K; IAP is the ion activity product and K is the equilibrium constant) were calculated using the computer program NETPATH (Plummer and others, 1994). The plot of SI values for CO_2 gas, calcite, and dolomite along the tracer reach (fig. F11) shows that the partial pressure of CO_2 is decreasing downstream from gaining reaches. Near-surface degassing of CO_2 appears to be the most important factor controlling the distribution of carbonate species along the study reach.

Spatial variations in the concentrations of the major anions—chloride, sodium, and sulfate (Cl^-, Na^+, and SO_4^{-2})

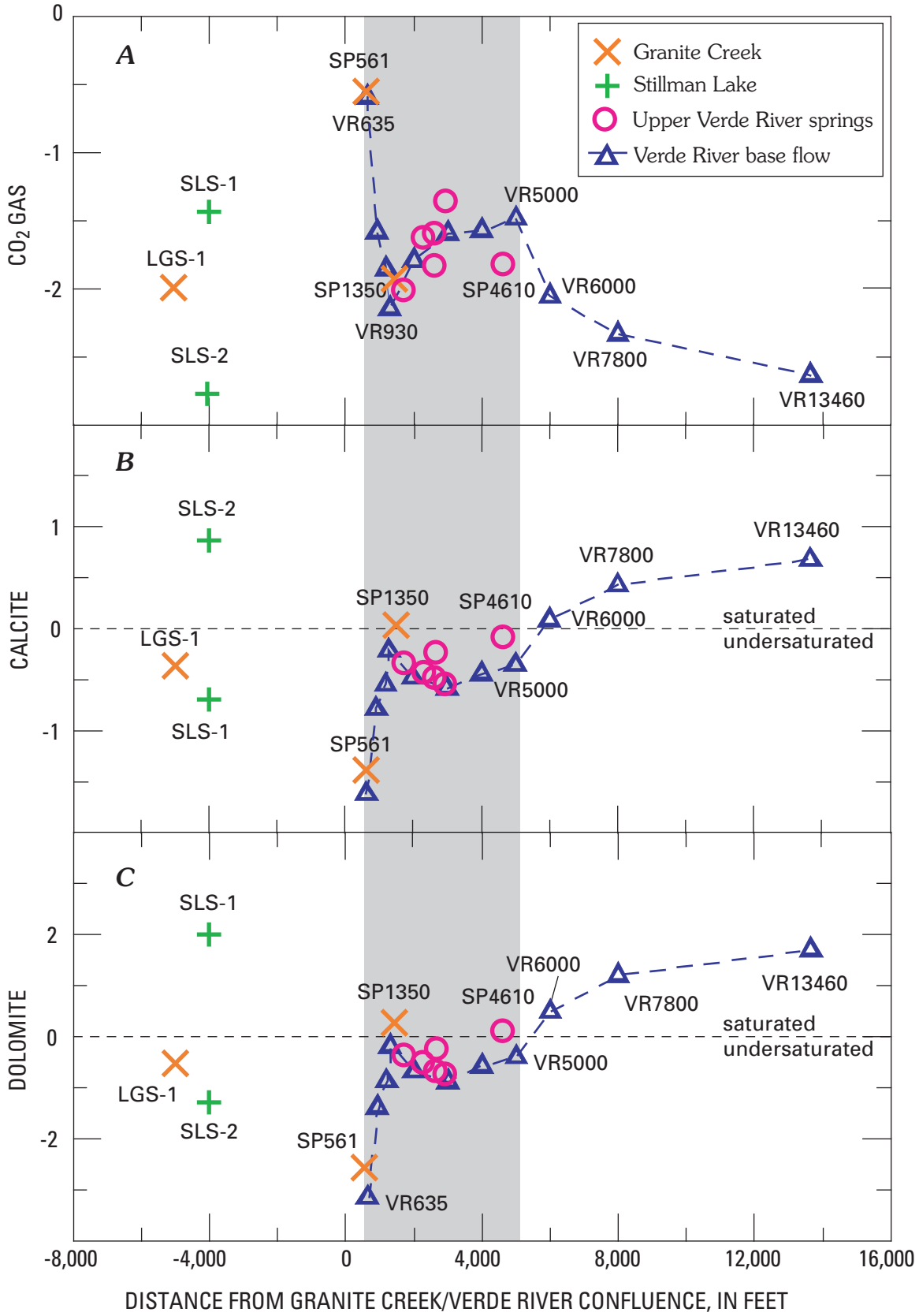

Figure F11. Graphs showing changes in saturation indices of (*A*) CO_2 gas, (*B*) calcite, and (*C*) dolomite versus distance from Granite Creek/Verde River confluence. Shaded area indicates extent of gaining reach.

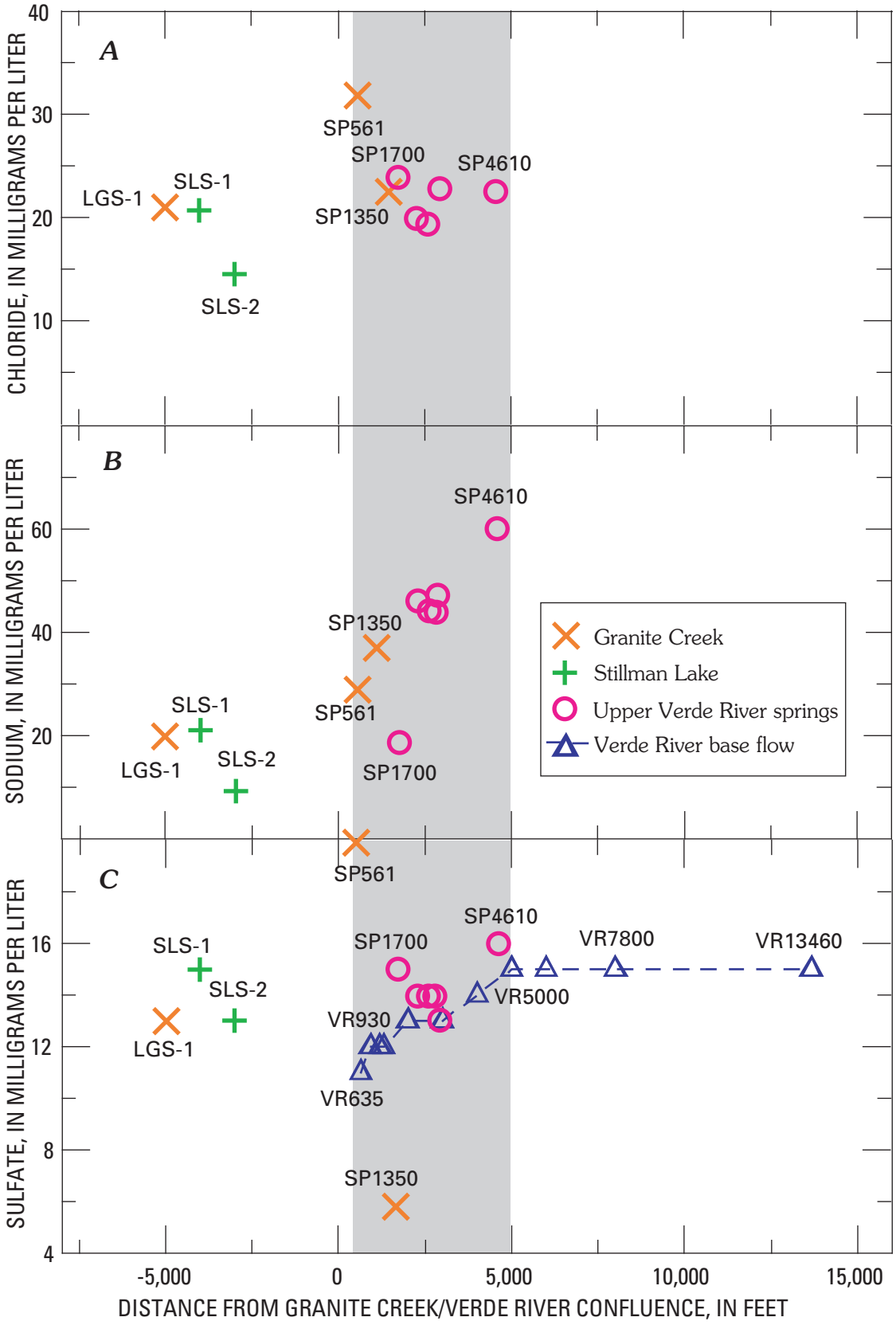

Figure F12. Graphs showing changes in (*A*) chloride, (*B*) sodium, and (*C*) sulfate versus distance from Granite Creek/Verde River confluence. Stream concentrations in the study reach are influenced by NaCl tracer and therefore instream values for Cl and Na are not shown. Shaded area indicates extent of gaining reach.

were plotted with distance along the tracer reach (fig. F12). Fortunately for the accuracy of the discharge calculations, background concentrations of chloride varied little, within a small range along the tracer reach, and the tracer reach values could be corrected for background contributions of chloride. The mean chloride concentrations for the upper Verde River springs network varied between 19.3 to 23.9 mg/L, with a mean concentration of 19.6 mg/L (n = 7). Del Rio Springs, Stillman Lake, and Granite Creek had chloride concentrations between 14.5 and 20.8 mg/L. Instream Cl^- and Na^+ concentrations in the Verde River were artificially influenced by the NaCl tracer and are not plotted in figure F13, although they are provided in table F1.

In contrast, Na^+ concentrations in discharge from upper Verde River springs varied between 37 and 60 mg/L. Contact with shale of marine origin containing rhyolitic ash (such as the Chino Valley Formation or playa sediment) is the most likely source of elevated concentrations of Na^+ (as well as As, B, Li, and K) in wells intercepting the D-C zone near the ground-water outlet of the Big Chino aquifer (Wirt and DeWitt, Chapter E, fig. E3, this volume). The Chino Valley Formation, where present, underlies the Martin Limestone and overlies the Tapeats Sandstone. The Chino Valley Formation is prominently exposed at the confluence of Stillman Lake and Granite Creek (southwest bank). It is thought to underlie the Martin Limestone beneath the north wall of the canyon and is the moswt likely source of dissolved Na^+ in discharge to upper Verde River springs. Sulfate concentrations were relatively low (between 6 and 16 mg/L) but increased over the tracer reach as a consequence of mixing between Little Chino ground water and upper Verde River springs. Sulfate concentrations in discharge from upper Verde River springs varied little, between 13 and 16 mg/L.

Selected Trace Elements

Elevated levels of boron (B) and lithium (Li) in upper Verde River springs are the highest in the headwaters region with the exception of the four Big Chino bedrock wells penetrating the D-C zone, described earlier in Chapter E. These bedrock wells have a distinct trace-element chemistry containing 330–460 µg/L of B and 54-86 µg/L of Li, respectively (Wirt and DeWitt, Chapter E, fig. E3; and Appendix A). The occurrence of these constituents is spatially associated with argillaceous rocks in the lower Paleozoic section. Strontium (Sr) is another trace element useful in indicating flowpath origin and is predominantly derived from the dissolution of feldspar minerals in igneous rocks (Wirt and DeWitt, Chapter E, fig. E3; and Appendix A). Some Sr also is present in carbonate rocks, but at relatively low levels in comparison to the Sr-rich volcanic rocks in the study area (Chapter E, this volume).

Concentrations of B and Li were lowest for Granite Creek and Stillman Lake samples but increased along the tracer reach more than threefold from 74 to 270 µg/L and from 15 to 49 µg/L, respectively (fig. F13). In contrast to Li and B, concentrations of Sr were highest in the Granite Creek and Stillman Lake samples (540 to 620 µg/L; n = 3). Strontium concentrations for upper Verde River springs samples were significantly lower, ranging between 360 and 440 µg/L Sr. The higher Sr concentrations are attributed to Little Chino source water in contact with Tertiary lati-andesite, whereas the Sr content in upper Verde River springs probably is related to contact with the Tertiary 5-mya basalt unit. Basalt flows partly cover the Paleozoic rocks in the confluence area and extend beneath surficial alluvial deposits in lower Big Chino Valley (fig. B8, Chapter B, this volume). The buried playa deposit in the center of Big Chino Valley is also a possible source of dissolved strontium along this flowpath.

Trace-element concentrations provide evidence for water-rock interactions along ground-water flowpaths. Elevated levels of B and Li are interpreted as having water/rock contact within the lower Martin/Chino Valley/Tapeats interface. High concentrations of Sr in Stillman Lake samples are interpreted as evidence for contact with volcanic igneous rocks along the ground-water outlet of northern Little Chino Valley.

Hydrogen and Oxygen Stable Isotopes

The composition of hydrogen and oxygen stable isotopes provides some of the most definitive geochemical evidence for identifying the source areas of springs and their aquifers. These isotopes are particularly useful in tracing ground-water flowpaths because they are part of the water molecule and can be assumed to behave conservatively once the water has reached the saturated zone and no longer has contact with the atmosphere. Evaporation and condensation of atmospheric precipitation and moisture in the unsaturated zone are the most significant physical processes that affect the proportions of these isotopes. The effects of evaporation were significant for most of the samples collected from Stillman Lake and, to a lesser degree, from lower Granite Creek. A discussion of the effects of evaporation has been presented in Chapter E (Wirt and DeWitt, this volume). In their figure E4, samples from Del Rio Springs, Granite Creek, and Stillman Lake plot along a dashed regression line with a slope of approximately 4, showing ground water similar to that discharging at Del Rio Springs (the major point of discharge for the Little Chino basin-fill aquifer) as the ground-water source for Stillman Lake and Granite Creek. This interpretation is corroborated by the slope of the water-level gradient from Del Rio Springs toward the confluence area (Wirt and others, Chapter D, this volume, fig. D7). Thus, it is evident that ground water discharging upgradient from the Granite/Verde confluence has been subjected to varying degrees of evaporation.

In figure F14, the stable-isotope samples plot into two main groups, with most of the samples from Stillman Lake and lower Granite Creek enriched by evaporation and comparatively heavier than samples from upper Verde River Springs. The "Little Chino" sample collected closest to the point where it emerged from the ground and least likely to have been affected by evaporation (with the exception of Del Rio Spring) was Lower Granite spring (site LGS-1; –9.7‰ $\delta^{18}O$ and –70‰

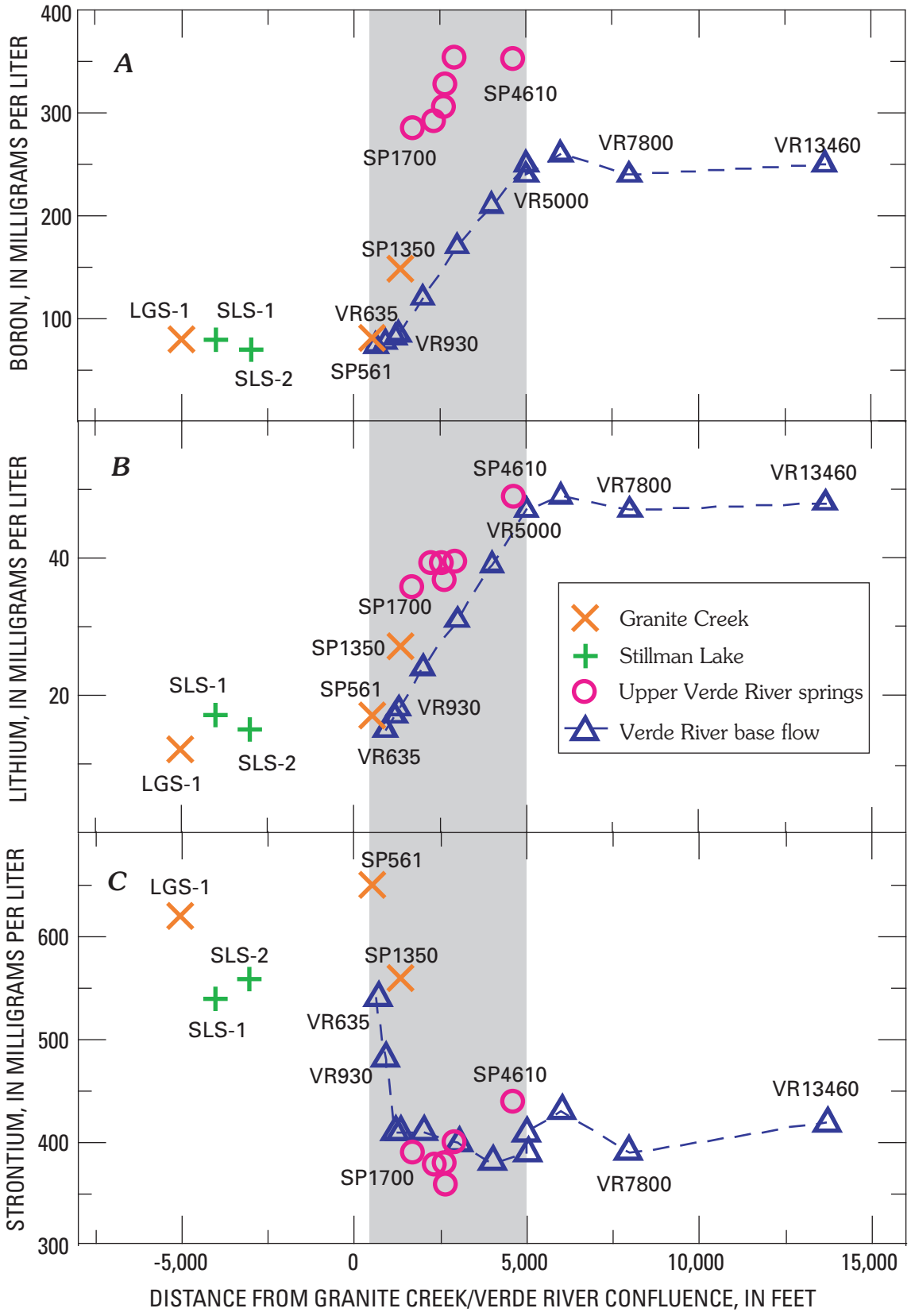

Figure F13. Graphs showing changes in (*A*) boron, (*B*) lithium, and (*C*) strontium versus distance from Granite Creek/Verde River confluence. Shaded area indicates extent of gaining reach.

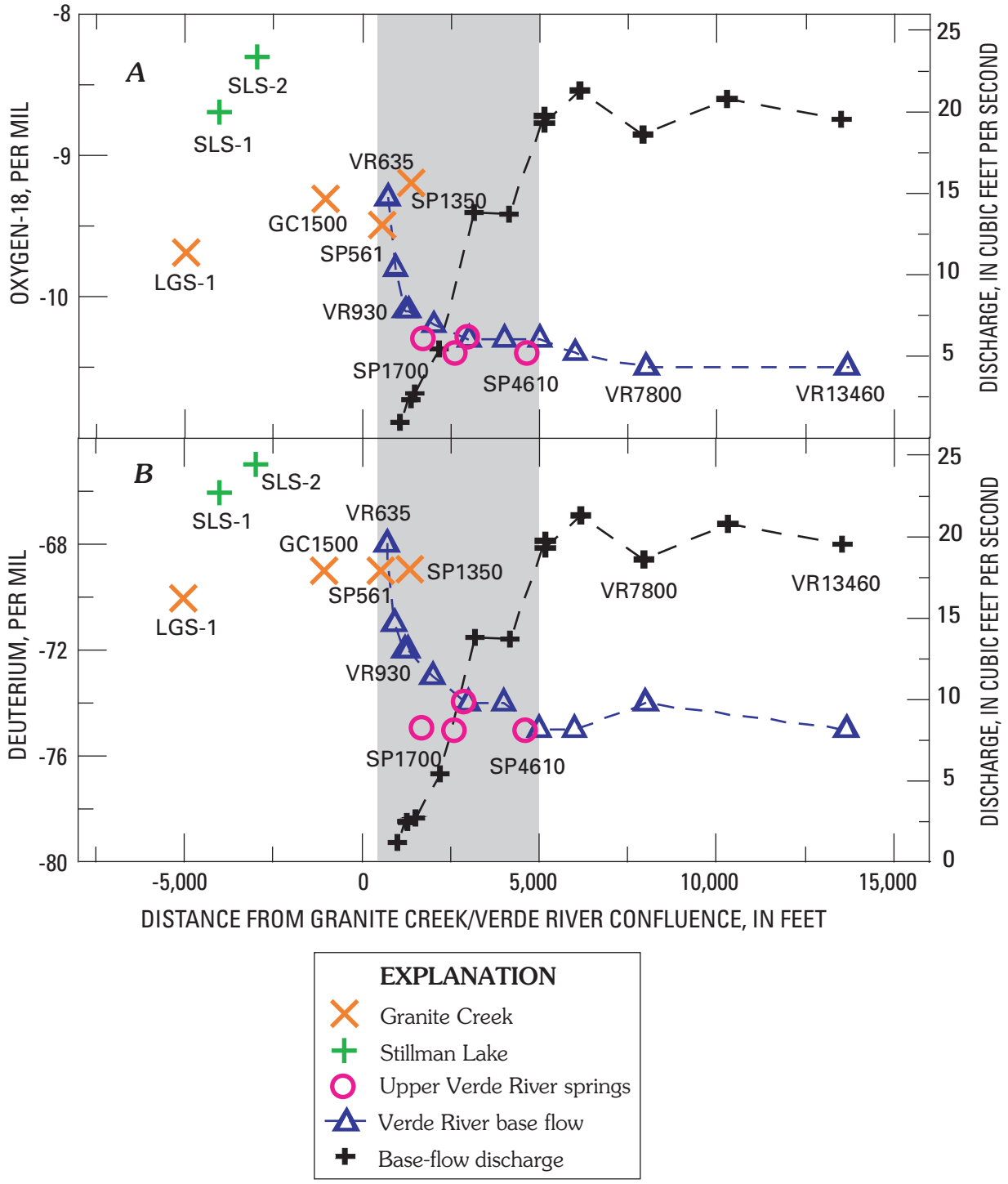

Figure F14. Graphs showing changes in stable isotopes (left axis) of (*A*) oxygen, and (*B*) hydrogen, and base flow (right axis) versus distance from Granite Creek/Verde River confluence. Shaded area indicates extent of gaining reach.

δD). In the uppermost reach of the Verde River, instream mixing of "Little Chino" sources of ground water with inflow from upper Verde River springs was the most important process downstream from site VR1200. The furthest point downstream from the confluence where Granite Creek inflow was identified was site SP1350, a small 3-ft radius pool that did not connect directly with the Verde River, at least on the ground surface. Based on supporting evidence from field-measured parameters (fig. F9) and the T3 automatic sampler (fig. F7), inflow from upper Verde River springs strongly emerges first in the vicinity of stream site VR1300. If one presumes that all inflow upgradient from site VR1200, with a discharge of 2.7±0.08 ft^3/s, originates as ground-water discharge from Granite Creek and Stillman Lake, then at least 13.8±0.7 percent of the total base flow of 19.5±1.0 ft^3/s at site VR13460 can be attributed to the Little Chino basin-fill aquifer.

Because the base flow of lower Granite Creek was about 0.5 ft^3/s, the remaining four-fifths of the 2.7±0.08 ft^3/s attributed the Little Chino aquifer is contributed along the Stillman Lake flowpath. This estimate is supported by the decrease in specific conductance between VR635 and VR1200, which shows mixing between the Stillman Lake and Granite Creek fractions (fig. F9 and table F1). The remaining 86.2 percent of total flow at Stewart Ranch is attributed to discharge from upper Verde River springs.

All lines of geochemical evidence show mixing between ground water from the Little Chino subbasin and upper Verde River springs immediately downstream from VR1200. At the lower end of the tracer reach, the $\delta^{18}O$ of the final base-flow mixture (–10.5+0.2‰ at site VR13460) should be intermediate to those for Lower Granite spring (site LGS-1, –9.7+0.2‰) and upper Verde River springs (site SP4610, –10.4+0.2‰). Instead, stream values for $\delta^{18}O$ and δD between sites VR6000 and VR13460 cannot be distinguished from those reported for upper Verde River springs, as they are within analytical precision of one another. This is an indication that mixing may have occurred with unsampled inflow that is isotopically depleted with respect to the sampled inflows.

Perhaps, the most notable attribute of the upper Verde River springs sample group is the relative lack of analytical variation (table F1, n = 5). Because some data from previous studies were analyzed by different laboratories, two standard-deviation analytical precisions of 0.2‰ for $\delta^{18}O$ and 2.0‰ for δD have been used for all of the stable-isotope data in this study (Kendall and Caldwell, 1998; p. 75; Christopher J. Eastoe, oral commun., 2003)—yet the upper Verde River springs samples from the synoptic sampling varied by less than 0.1‰ for $\delta^{18}O$ and 1.0‰ for δD. Differences between upper Verde River springs and the final base-flow mixture at Stewart Ranch (site VR-13460) differ within the margin of analytical uncertainty, which is about 15 percent. Mixing could be occurring at the scale of this uncertainty, but the amount cannot be determined with any confidence solely based on the stable-isotope results.

Wirt and DeWitt (Chapter E, this volume, table E2) show that the carbonate aquifer north of the Verde River (M-D sequence) is substantially depleted (about 1.3+0.2 ‰) in $\delta^{18}O$ relative to upper Verde River springs. Although none of the samples from upper Verde River springs were more depleted in $\delta^{18}O$ and δD than samples of base flow at Stewart Ranch, some mixing of Big Chino ground water with isotopically depleted ground water as unsampled inflow appears likely. Inverse geochemical modeling is used next to evaluate the degree of mixing between the Big Chino basin-fill aquifer and the M-D sequence of the carbonate aquifer to produce the water chemistry observed at upper Verde River springs.

Inverse Geochemical Modeling to Determine Mixing Proportions at Upper Verde River Springs

The hypothesis that upper Verde River springs is a mixture of ground water from the Big Chino basin-fill aquifer and the carbonate aquifer was tested by inverse geochemical modeling using the computer program PHREEQC (Parkhurst and Apello, 1999). Inverse modeling uses existing geochemical analyses to account for chemical changes occurring as water evolves along a flowpath. Given two water analyses representing the starting and ending water composition along a flow path, inverse modeling will calculate the moles of minerals and gases that must enter or leave solution to account for differences in composition (Parkhurst and Apello, 1999). If two or more initial waters mix and subsequently react, PHREEQC computes the mixing proportion and the net geochemical reactions to account for the observed composition of the final water. Every possible geochemical mass-balance reaction is examined between selected evolutionary waters for a set of chemical and isotopic constraints and a set of plausible phases in the system. This modeling approach has been described extensively by Parkhurst and Plummer (1993) and Appelo and Postma (1999).

An advantage of PHREEQC (Version 2; Parkhurst and Apello, 1999) over earlier versions of PHREEQC and NETPATH (Plummer and others, 1994) is the capability to consider uncertainties associated with individual element analyses (Glynn and Brown, 1996). The user is allowed to specify the analytical uncertainty range for each element or isotope entered in the model. In addition, PHREEQC will determine mass-transfer models that minimize the number of phases involved, referred to as "minimal models." Unlike earlier mass-balance programs, PHREEQC includes a charge-balance constraint and water mass-balance constraint that allow additional adjustments to analytical element concentrations, alkalinity, and pH. These additional constraints are equivalent to including a mass balance on hydrogen or oxygen for changes that may result from water derived from mineral reactions, evaporation, or dilution.

In this study, PHREEQC was used (a) to calculate saturation indices and the distribution of aqueous species, (b) to identify net geochemical mass-balance reactions between initial and final waters along the outlet flowpath, and (c) to

calculate proportions of water types contributing to the final mixture. Extensive knowledge of the geologic framework and the geochemical system (detailed in Chapters D and E and the preceding part of this chapter) as well as an evaluation of cation-anion balances for individual wells was used to select representative initial and final waters for this modeling exercise. In brief, multiple flow lines within the lower Big Chino basin-fill aquifer converge toward Paulden (fig. F15; and fig. E9 of Chapter E, this volume) and the main flowpath continues through the D-C zone of the carbonate aquifer (well F) to upper Verde River springs (site G, fig. F15; sample SP1700, table F1). Well F is screened in a basalt-filled paleochannel north of the upper Verde River (Chapter B, fig. B8A; Chapter D, fig. D8) and occupies an intermediate location along the basin outlet flowpath (fig. F15).

In this exercise, mixing of four initial waters is allowed to occur between Paulden and upper Verde River springs (table F2, fig. F15). Initial waters include (a) well H representing the D-C zone of the regional carbonate aquifer underlying basin-fill alluvium near the outlet, (b) well E, representing basin alluvium and basalt facies of the Big Chino basin-fill aquifer near its outlet, (c) well F representing the carbonate aquifer between Big Chino Valley and upper Verde River springs, and (d) well M representing the M-D sequence of the carbonate aquifer north of the Verde River near Drake. The final endpoint is represented by ground water at spring G, which was the largest discrete spring in the upper Verde River springs network identified at the time of the synoptic sampling (site SP1700, table F1). All of the selected analyses have cation-anion balances lower than 5 percent.

The first step in inverse modeling was to examine trends in the water chemistry and thermodynamic state of the initial and final waters used in the model (tables F2 and F3). The most significant change between ground water near Paulden (well E) and upper Verde River springs (spring G) is a 91 percent increase in dissolved silica, as well as large increases in the concentrations of sodium (78 percent), boron (86 percent), and lithium (65 percent), as shown by the last column in table F2. In comparison, concentrations of calcium, magnesium, and sulfate increased slightly by 11 percent, 19 percent, and 21 percent; respectively. The only decreasing trend between well E and spring G was for strontium (–6.5 percent), which behaves independently of the other dissolved constituents discussed here.

Saturation indices (SIs) shown in table F3 indicate that calcite and dolomite are near or at saturation and that gypsum is undersaturated in all of the selected samples. Amorphous SiO_2 (chalcedony) is near saturation or slightly undersaturated in the regional carbonate aquifer (wells H and M), but slightly oversaturated in the basin-fill aquifer and upper Verde River springs (well E and spring G). Trends for SIs of Mg-silicate minerals, such as talc and sepiolite, strongly correlate with those for chalcedony, consistent with one or more of a family of related secondary silicate minerals dissolving along the outlet flowpath.

Water chemistry for well F is quite different from that for well H, although both wells are considered part of the D-C zone. Ground water underlying the margin of the Big Chino basin-fill aquifer at well H is near saturation with respect to celestite, chalcedony, calcite, and dolomite (table F3). Well H also has the highest concentrations of HCO_3^-, Ca^{+2}, Na^+, SO_4^{-2}, Cl^-, Li, and B and is moderately depleted in $\delta^{18}O$ and δD (table F2). In contrast, well F has dissolved-element concentrations far more similar to well E than well H, with the exception of silica. A trend of increasing silica from 22 to 44 mg/L from well E to well F is consistent with an abrupt change in rock type from basin-fill alluvium to fractured basalt. The silica concentration at well F is nearly the same as that at upper Verde River springs (spring G), indicating that a large fraction of the ground water discharging at upper Verde River springs evidently has been in contact with basalt, despite the observation of ground water emerging from limestone. The basalt paleochannel is interpreted as a preferential conduit for ground water movement in the local vicinity of well F.

In comparison to other samples along the ground-water outlet, the M-D sequence (represented by well M near Drake) had the lowest concentrations of Li and B and was the most depleted in $\delta^{18}O$ and δD. Stable-isotope compositions of oxygen and hydrogen usually are one of the best geochemical constraints in mass-balance calculations, but their application may be limited by the range of spatial variation, seasonal variation, or analytical uncertainty, which may allow for multiple nonunique solutions. Because a multitude of mixing scenarios or flowpaths can produce the same observed water chemistry, uncertainty limits were placed on all constituents used in the model to better constrain the number of possible reactions and more accurately determine the fractions of mixing solutions.

A global uncertainty of ±5 percent was assigned to all of the major and most of the trace-element analyses, consistent with cation-anion balances of less than ±5 percent (table F2). A larger uncertainty of ±10 percent was assigned to boron and lithium because they are known to behave nonconservatively in this system. Stable isotopes of oxygen, hydrogen, and carbon were assigned an uncertainty of 0.1‰ $\delta^{18}O$, 1.0‰ δD, and 2.0‰ $\delta^{13}C$, respectively (consistent with their reported analytical uncertainty for these analyses in this study). Calcite and dolomite mineral phases were assigned a value of –2.0‰ $\delta^{13}C$, based on a mean value of –1.85‰ (n = 36) for analyses of nearly pure limestone samples from the Redwall Limestone in north central Arizona (Muller and Mayo, 1986). Carbon-dioxide gas was assigned a value of –18.0‰ $\delta^{13}C$, based on the results of soil-gas samples collected from the Dripping Springs basin in central Arizona (Pierre Glynn, unpub. data, oral commun., 2005). The “minimal” option in PHREEQC was chosen to reduce the number of possible models and to provide only those models which are a best fit to the input data. In selecting this option, it is presumed that the simplest, least complicated models with the fewest phases are the most plausible models.

The model was required to evaluate mass transfers of the following 9 phases, which were chosen based on relative

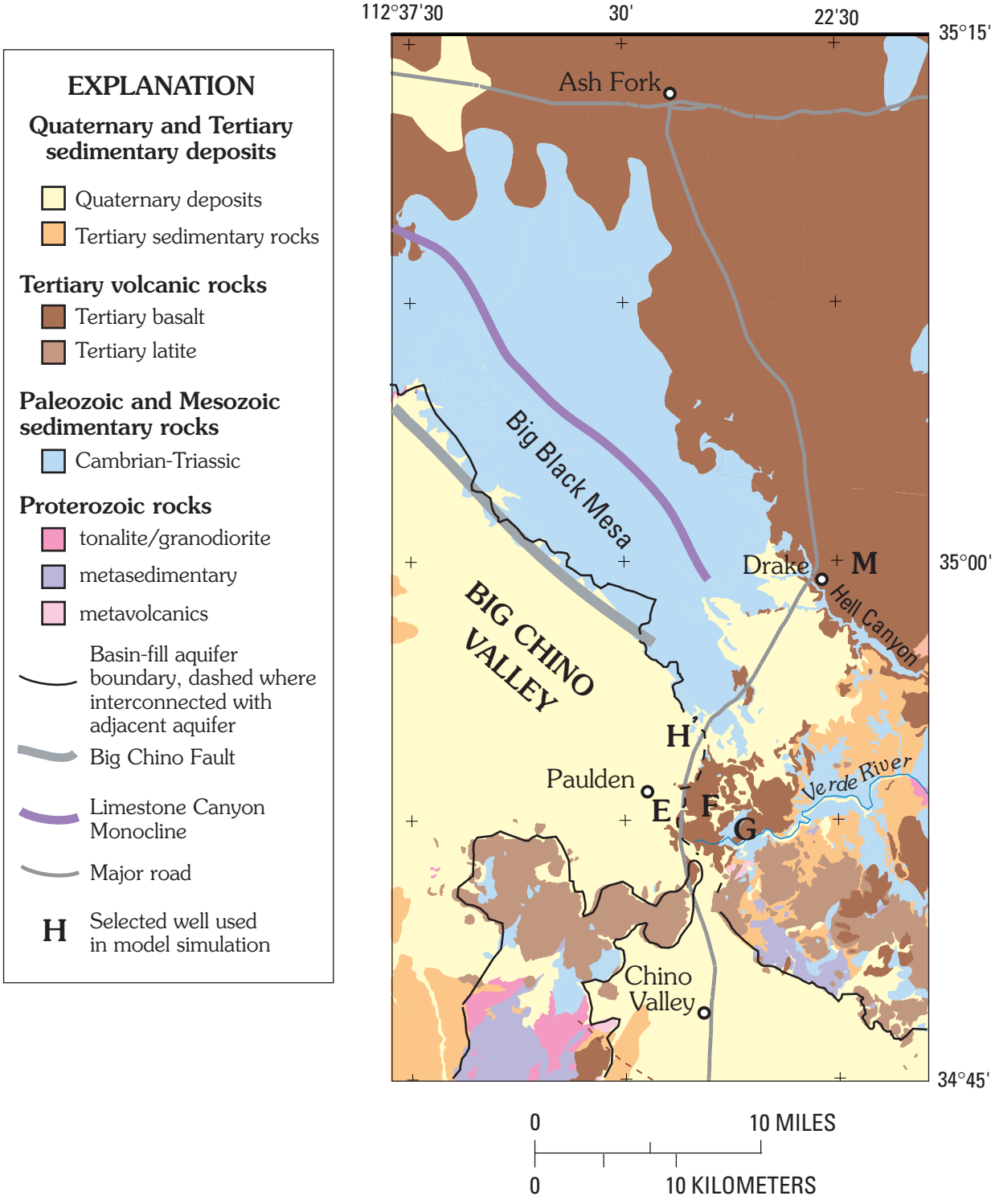

Figure F15 Geology map showing the location of selected wells and springs used in inverse geochemical modeling of Big Chino basin outlet flowpath (geology simplified from DeWitt and others, in press). Base is from U.S. Geological Survey digital data 1:100,000.

Table F2. Chemical composition of selected ground waters from the Verde River headwaters representing the Big Chino basin-fill aquifer, the regional carbonate aquifer (D-C zone and M-D sequence) and upper Verde River springs. Sample locations shown on Figure F15.
[Concentrations in mg/L; isotopes expressed in per mil, and pH in pH units; δ, delta; °C, centigrade]

	Well E	Well H	Well M	Well F	Spring G	Change between well E and spring G (%)
	Big Chino basin-fill aquifer near outlet	D-C zone beneath basin-fill aquifer	M-D sequence near Drake	D-C zone along main flowpath	Upper Verde River springs	
pH	7.8	7.0	7.7	7.7	7.8	
Dissolved oxygen	8.9	5.7	5.1	4.7	5.0	
Temperature (¡C)	18.7	25.9	23.6	18.2	19	
Alkalinity (as HCO_3)	195	500	220	235	256	
Calcium	36	64	40	41	40	11
Magnesium	16	28	19	18	19	19
Sodium	18	93	6	21	32	78
Silica (as SiO_2)	22	17	9	44	42	91
Strontium	0.370	0.350	0.101	0.408	0.346	-6.5
Sulfate	9.2	23	18	12	11.1	21
Chloride	13	27	7	15	17	31
Lithium	0.017	0.086	0.003	0.019	0.028	65
Boron	0.073	0.440	0.012	0.088	0.136	86
^{18}O	-10.3	-10.7	-10.9	-10.2	-10.3	
^{2}H	-73	-77	-80	-73	-75	
^{13}C	-8.2	-5.6	-2.0	-8.8	-7.0	
Cation/Anion balance percent error	1.68	0.38	-4.72	-1.00	0.43	

Table F3. Saturation indices for mixing endpoints contributing to upper Verde River springs. Positive numbers indicate saturation, negative numbers indicate undersaturation. Sample locations shown on Fig. F15.
[NC, not calculated]

		Well E	Well H	Well M	Well F	Spring G
Mineral phases	Chemical formula	Big Chino basin-fill aquifer near outlet	D-C zone beneath basin-fill aquifer	M-D sequence near Drake	D-C zone along main flowpath	Upper Verde River springs
Calcite	$CaCO_3$	0.12	0.00	0.18	0.14	0.27
Dolomite	$CaMg(CO_3)_2$	0.16	0.00	0.37	0.18	0.49
Strontianite	$SrCO_3$	-1.38	-1.82	-1.96	-1.37	-1.21
Gypsum	$CaSO_4 : 2H_2O$	-2.83	-2.34	-2.52	-2.68	-2.74
Celestite	$SrSO_4$	-3.12	-0.01	-3.41	-2.98	-3.1
Chalcedony	SiO_2	0.19	-0.01	-0.26	0.5	0.46
SiO_2 (amorphous)	SiO_2	-0.67	-0.84	-1.10	-0.37	-0.4
Sepiolite	$Mg_2Si_3O_{7.50}H : 3H_2O$	-1.7	-4.70	-3.01	-1.13	-0.74
Talc	$Mg_3SSi_4O_{10}(OH)_2$	0.93	-2.96	-0.46	1.6	2.26
Halite	NaCl	-8.18	-7.19	-8.94	-8.05	-7.82
Albite	$NaAlSi_3O_8$	NC	NC	NC	NC	NC
Anorthite	$CaAl_2Si_2O_8$	NC	NC	NC	NC	NC
Kaolinite	$Al_2Si_2O_5(OH)_4$	NC	NC	NC	NC	NC
Carbon dixoide	CO_2 (gas)	-2.56	-1.32	-2.38	-2.38	-2.44

Table F4. Results of PHREEQC phase mole transfers and mixing model simulations for upper Verde River springs.

Model no.	Phase Mole Transfers*									No. of phases	Sum of residuals
	SiO_2 Chalcedony	CO_2 (gas)	NaCl Halite	$CaMgCO_3$ Dolomite	$Mg_3Si_4O_{10}(OH)_2$ Talc	$CaCO_3$ Calcite	$CaSO_4$ Gypsum	CaF_2 Fluorite	$SrSO_4$ Celestite		
1		-2.31E-04					-2.94E-05	-2.89E-06		3	1.14E+01
2			8.42E-05		2.50E-05			-3.31E-06	-8.50E-07	4	1.78E+01
3	1.00E-04	-1.66E-04	8.42E-05					-3.31E-06	-8.50E-07	5	1.70E+01
4				6.03E-05			-2.94E-05	-3.09E-06	-5.78E-07	4	1.87E+01
5					2.49E-05		-2.17E-05	-3.53E-06		3	1.50E+01
6	1.00E-04		8.42E-05	5.69E-05				-3.31E-06	-8.50E-07	5	2.05E+01
7	1.27E-04			6.47E-05			-2.82E-05	-3.82E-06		4	1.97E+01
8			7.97E-05	5.41E-05			-3.50E-05	-1.93E-06		4	2.24E+01
9					2.25E-05		-2.31E-05	-2.65E-06	-6.25E-07	4	1.48E+01
10					2.04E-05	1.48E-05	-2.91E-05	-2.49E-06		4	1.71E+01
11			3.17E-05		2.16E-05		-2.67E-05	-2.27E-06		4	1.59E+01
12		-2.22E-04					-2.44E-05	-2.87E-06	-6.18E-07	4	7.88E+00
13			4.80E-05	5.17E-05			-2.58E-05	-2.02E-06	-6.44E-07	5	1.73E+01

*Results in millimoles per kilogram of H_2O. Positive numbers indicate moles entering solution, negative numbers indicate moles leaving solution owing to precipitation or degassing. Sample locations are shown on figure F15.

Model no.	Solution Fractions for Initial Waters													Final water
	Devonian-Cambrian Zone north of Paulden			Big Chino basin-fill aquifer at outlet near Paulden			Carbonate aquifer between Big Chino outlet and Verde River near Paulden			Sum of Big Chino initial waters	Carbonate aquifer north of upper Verde River (Mississippian-Devonian sequence)			
	Well H	Min	Max	Well E	Min	Max	Well F	Min	Max	H + E + F	Well M	Min	Max	
1	0.14	0.12	0.15	0.00	0.00	0.00	0.79	0.79	0.82	0.94	0.06	0.05	0.07	1.00
2	0.10	0.09	0.10	0.25	0.24	0.25	0.66	0.66	0.66	1.00	0.00	0.00	0.00	1.00
3	0.10	0.09	0.10	0.25	0.24	0.25	0.66	0.66	0.66	1.00	0.00	0.00	0.00	1.00
4	0.12	0.11	0.12	0.12	0.09	0.13	0.76	0.75	0.79	1.00	0.00	0.00	0.00	1.00
5	0.13	0.12	0.15	0.16	0.05	0.23	0.67	0.56	0.77	0.96	0.04	0.03	0.08	1.00
6	0.10	0.09	0.10	0.25	0.24	0.25	0.66	0.66	0.66	1.00	0.00	0.00	0.00	1.00
7	0.13	0.13	0.13	0.23	0.22	0.23	0.61	0.60	0.62	0.97	0.03	0.03	0.04	1.00
8	0.10	0.10	0.10	0.00	0.00	0.00	0.83	0.82	0.84	0.93	0.07	0.06	0.08	1.00
9	0.13	0.11	0.13	0.00	0.00	0.00	0.87	0.87	0.89	1.00	0.00	0.00	0.00	1.00
10	0.13	0.12	0.13	0.00	0.00	0.00	0.81	0.80	0.82	0.94	0.06	0.06	0.08	1.00
11	0.12	0.10	0.12	0.00	0.00	0.00	0.82	0.76	0.84	0.94	0.06	0.06	0.12	1.00
12	0.14	0.11	0.18	0.00	0.00	0.00	0.86	0.82	0.89	1.00	0.00	0.00	0.00	1.00
13	0.10	0.09	0.11	0.00	0.00	0.00	0.90	0.89	0.91	1.00	0.00	0.00	0.00	1.00

activities of major and trace dissolved species and on the calculated values of the SIs:

calcite (dissolution only)
dolomite (dissolution only)
chalcedony
CO_2 gas (exsolution only)
halite
talc
gypsum
fluorite
celestite

Calcite, dolomite, and quartz (chalcedony) are common rock-forming minerals in basin-fill alluvium, as well as in igneous and sedimentary rocks. As shown in fig. F11, CO_2 gas is an important phase for near-surface carbonate reactions. Gypsum and halite are common secondary minerals that were included to account for the presence of SO_4, Na, and Cl, although other sources are possible. Similarly, fluorite is needed to provide a fluoride-bearing phase. Celestite was included to provide a strontium-bearing phase, and its presence is supported by SI data for well H (table F3). Saturation indices for common alumina-silicate minerals such as albite, anorthite and kaolinite were *not* calculated by the model because too little dissolved aluminum is present. Alternately, a nonaluminous mineral such as talc or sepiolite was selected to provide a Mg-silicate phase. Talc includes of a large family of minerals such as chlorite, mica, phyllite, or clays formed by alteration of igneous rocks. In addition, the model allows cation exchange to occur between Ca and Na.

Within the above constraints, thirteen plausible minimal models were identified by PHREEQC (table F4). It is noted that linear combinations of these models also represent possible models, and that by assigning larger uncertainties to the constraints, there could be a much greater number of nonunique models. The models shown here are the simplest models yielding the best fit for the given analytical data and the designated constraints.

All of the minimal models presented in table F4 require between three and five phase transfers. A few of the models call upon relatively large phase transfers of chalcedony or degassing of carbon-dioxide. Nearly half the models require phase transfers involving dissolution of halite, dolomite, or talc. All models include minor transfers of fluorite, and most of the models require minor transfers of gypsum and/or celestite. The fact that calcite is included in only one of the models is an important result indicating that other processes than carbonate dissolution are more likely to have an effect on concentrations of Ca^{+2} and Mg^{+2} along the outlet flowpath. This result is somewhat surprising, given the extensive exposure to limestone (and dolomite) along the outlet flowpath. For all of the models presented in table F4, the range of variability in the calculated uncertainty (sum of residuals) is within 3.5 percent. None of the models are favored over any of the other possible models; all are considered plausible.

Six out of thirteen minimal models support a small amount of mixing between Big Chino ground water and the M-D sequence of the carbonate aquifer. The sum of three initial waters from Big Chino Valley (wells H, E, and F) accounts for between 93 and 100 percent of total discharge at upper Verde River springs, with the M-D sequence outside of Big Chino Valley accounting for none to a maximum of 7 percent of total spring inflow. At the Big Chino outlet near Paulden (well H in table F4), the D-C zone of the underlying carbonate aquifer contributes on the order of 10 to 15 percent of the ground water discharging from Big Chino Valley.

In summary, all thirteen of the minimal inverse models are consistent with converging flow along the valley outlet near Paulden to produce the water chemistry at upper Verde River springs by means of one or more of the following processes: (a) near-surface degassing of carbon dioxide, (b) dissolution of silicate minerals, (c) precipitation of gypsum, or (d) dissolution of small amounts of relatively common minerals such as halite, dolomite, talc, or calcite. All of these possible model scenarios are accompanied by a minor phase transfer of fluorite and usually one of celestite. Despite contact with carbonate minerals, the models predict relatively little change in the saturation state of calcite and dolomite along the Big Chino basin outlet flowpath, contrary to what might be expected for evolution along a carbonate aquifer flowpath. Compositional variations in major dissolved species such as Ca^{+2}, Mg^{+2}, and HCO_3^- can be entirely accounted for by simple mixing and water interaction with non-carbonate minerals. No mixing with the M-D sequence of the carbonate aquifer is necessary to account for the water chemistry at upper Verde River springs, although a small fraction (less than 7 percent) is plausible.

Summary and Conclusions

Using the tracer-dilution method, base flow at Stewart Ranch during low-flow conditions of June 2000 was measured as 19.5±1.0 ft^3/s. Most ground-water inflow to upper Verde River springs occurs within the first mile downstream from the mouth of Granite Creek. Base flow in the upper Verde River upstream from Stewart Ranch is predominantly derived from upper Verde River springs (86.2 percent) and, to a lesser extent, from the Little Chino basin-fill aquifer. The Little Chino basin-fill aquifer contributed 13.8±0.7 percent of the base flow (2.7±0.08 ft^3/s) based on the trace-dilution approach. Approximately four-fifths of the Little Chino inflow appears to originate from beneath Stillman Lake, as opposed to from lower Granite Creek which had a base flow of about 0.5 ft^3/s upstream from its mouth.

Inverse model simulations in PHREEQC indicate that discharge to upper Verde River springs upstream from Stewart Ranch is predominantly derived from mixing of initial water sources solely within Big Chino Valley. A small amount of mixing with the M-D sequence north of the Verde River is possible (less than about 7 percent), although none is required

by a majority of the model simulations. A potential contribution from the M-D sequence (if any) would be credited to the part of the carbonate aquifer north of the upper Verde River between Big Black Mesa and lower Hell Canyon. These model results are consistent with the Big Chino basin-fill aquifer and the D-C zone of the carbonate aquifer being strongly interconnected near the basin outlet and functioning together as a single source of ground water from beneath Big Chino Valley.

The contributions to the base flow at the Paulden gauge can be estimated by using a simplifying assumption. An additional 7 percent of Verde River base flow is contributed between Stewart Ranch and the Paulden gauge. The source of this inflow has not been determined, but a reasonable simplifying assumption is that the sources of inflow for the remaining 7 percent are in the same proportion as those at Stewart Ranch. This assumption is supported by relatively little variation in the stable-isotope composition of streamflow between Stewart Ranch and the Paulden gauge. The readjusted contributions from each aquifer source at the Paulden gauge are as follows: (a) Little Chino basin-fill aquifer, 14 percent; (b) M-D sequence north of the Verde River, less than 6 percent; and (c) the combined Big Chino basin-fill aquifer and D-C zone of the underlying carbonate aquifer, greater than 80 to as much as 86 percent.

The model estimates for the ground-water fraction from the M-D sequence north of the upper Verde River compares favorably with the estimate by Ford (2002), who determined recharge from the geographical area underlying Big Black Mesa at about 5 percent of the base flow at the Paulden gauge using nongeochemical methods. The M-D sequence is part of a 3-dimensional regional aquifer, whereas the Big Black Mesa defined by Ford (2002) is a geographical area. A contribution of about 5 percent from the M-D sequence seems entirely consistent with the conceptual geologic framework of the carbonate aquifer developed in the earlier chapters of this report.

In summary, the accuracy of the inverse model simulations depends on how well the selected initial waters and mineral phases reflect the mineralogy and water chemistry of the water-bearing units. A large number of nonunique models are possible, although only the best-fit "minimal" models for the data have been presented here. Important reactions identified by inverse modeling include the dissolution of silicates and degassing of carbon dioxide, processes supported by field and analytical data. The most likely cause of a two-fold increase in dissolved silica is water-rock interaction with the basalt-filled paleochannel east of Paulden. Variations in pH and bicarbonate along the tracer reach primarily are attributed to degassing of CO_2 where ground water is discharging to land surface. Calcite and dolomite minerals remain near or at saturation along the length of the basin outlet flowpath, indicating that the dissolution (or precipitation) of carbonate rocks is *not* a dominant process, despite extensive exposure to limestone and dolomite.

In conclusion, the water chemistry of upper Verde River springs is consistent with the evolution of ground water from the Big Chino basin-fill aquifer that has traveled a short distance through the carbonate aquifer to emerge in the upper Verde River canyon. Little or no mixing with ground water from the M-D sequence of the carbonate aquifer north of the upper Verde River is required to create the water chemistry at upper Verde River springs. Inverse geochemical modeling constrains the potential contribution from the M-D sequence of the regional carbonate aquifer to less than about 6 percent of base flow at the Paulden gauge. Other lines of nongeochemical evidence indicate that a contribution on the order of about 5 percent is plausible, but uncertain. Adjusted contributions from each aquifer source to base flow at the Paulden gauge are estimated as: (a) Little Chino basin-fill aquifer, 14 percent; (b) M-D sequence north of the Verde River, less than about 6 percent; and (c) the combined Big Chino basin-fill aquifer and underlying D-C zone of the carbonate aquifer, at least 80 to 86 percent.

References Cited

Anderson, T.W., 1976, Evapotranspiration losses from floodplain areas in Central Arizona: U.S. Geological Survey Open-File Report 76-864, 91 p.

Appelo, C.A.J., and Postma, D., 1999, Geochemistry, Groundwater, and Pollution: Balkema, Rotterdam, 536 p.

Bencala, K.E., McKnight, D.M., and Zellweger, G.W., 1990, Characterization of transport in an acidic and metal-rich mountain stream based on a lithium tracer injection and simulations of transient storage: Water Resources Research, v. 26, no. 5., p. 989–1000.

Betancourt, J.L, 2003, The current drought (1999–2003) in historical perspective: 2003 Southwest Drought Summit report, May 12–13, 2003, Northern Arizona University, Flagstaff, Arizona, *http://www.mpcer.nau.edu/*, accessed on May 19, 2004.

Boner, F.C., Davis, R.G., and Duet, N.R., 1991, Water resources data, Arizona, water year 1991: U.S. Geological Survey Water-Data Report AZ-91-1.

Briggs, P.H., and Fey, D.L., 1996, Twenty-four elements in natural and acid mine waters by inductively coupled plasma-atomic emission spectrometry, *in* Arbogast, B.F., ed., Analytical methods manual for the Mineral Resources Surveys Program: U.S. Geological Survey Open-File Report 96–525, p. 95–101.

Broshears, R.E., Bencala, K.E., Kimball, B.A., and McKnight, D.M., 1993, Tracer-dilution experiments and solute-transport simulations for a mountain stream, Saint Kevin Gulch, Colorado: U.S. Geological Survey Water-Resources Investigations Report 92–4081, 18 p.

Bullen, T.D., and Kendall, Carol, 1998, Tracing of weathering reactions and water flowpaths: A multi-isotope approach, *in* Kendall, Carol and McDonnell, J.J., eds., Isotope Tracers in Catchment Hydrology: Elsevier, New York, p. 611–646.

d'Angelo, W.M., and Ficklin, W.H., 1996, Fluoride, chloride, nitrate, and sulfate in aqueous solution by chemically suppressed ion chromatography, *in* Arbogast, B.F., ed., Analytical methods manual for the Mineral Resources Surveys Program: U.S. Geological Survey Open-File Report 96-525, p. 149–153.

DeWitt, Ed, Langenheim, V.E., Force, Eric, Vance, Kelley, and Lindberg, P.A., *with* a digital database by Doug Hirschberg, Guy Pinhassi, and Nancy Shock, in press, Geologic map of the Prescott National Forest and headwaters of the Verde River, Yavapai and Coconino Counties, Arizona, U.S. Geological Survey Miscellaneous Investigations Map, scale 1:100,000, two sheets.

Dodder, Joanna, 2004, Study supports Big Chino contribution to river: The Daily Courier, April 22, 2004, Prescott, Arizona, p. 12A.

Ewing, D.B., Osterberg, J.C., and Talbot, R.W., 1994, Groundwater Study of the Big Chino Valley—Hydrology and hydrogeology: Bureau of Reclamation Technical Report, Denver, Colorado, 14 p. plus 6 appendixes.

Fisk, G.G., Duet, N.R., Evans, D.W., Angeroth, C.E., Castillo, N.K., and Longsworth, S.A., 2004, Arizona Water Resources Data—Water Year 2003: U.S. Geological Survey Water-Data Report AZ-03-1, 328 p.

Ford, J.R., 2002, Big Chino Valley ground water as the source of the Verde River, *in* Ground Water/Surface Water Interactions, July 1–3, 2002: American Water Resources Association summer specialty conference, 6 p.

Freethey, G.W., and Anderson, T.W., 1986, Predevelopment hydrologic conditions in the alluvial basins of Arizona and adjacent parts of California and New Mexico: U.S. Geological Survey Hydrologic Investigations Atlas HA–664.

Glynn, Pierre, and Brown, James, 1996, Reactive transport modeling of acidic metal-contaminated ground water at a site with sparse spatial information, *in* Steefer, C.I, Lichtner, P., and Oelkers, E., eds., Reviews in Mineralogy: Mineralogical Society of America, Washington, D.C., v. 34, p. 377–438.

Hem, J.D., 1992, Study and interpretation of the chemical characteristics of natural water: U.S. Geological Survey Water-Supply Paper 2254, 263 p.

Hendrickson, Raquel, 2000, USGS report creates waves—Government agencies fence over Verde source: Verde Independent, Camp Verde, Arizona, (*http://www.verdevalleynews.com* on December 18, 2000).

Hereford, Richard, 1975, Chino Valley Formation (Cambrian?) in northwestern Arizona: Geological Society of America Bulletin, v. 86, p. 677–682.

Horowitz, A.J., Demas, C.R., and Fitzgerald, K.K., 1994, U.S. Geological Survey protocol for the collection and processing of surface-water samples for the subsequent determination of inorganic constituents in filtered water: U.S. Geological Survey Open-File report 94–539, 157 p.

Kendall, Carol, and Caldwell, E.A., 1998, Fundamentals of isotope geochemistry, *in* Kendall, Carol and McDonnell, J.J., eds., Isotope tracers in catchment hydrology: Elsevier, New York, Chapter 3, p. 51–86.

Kimball, B.A., 1997, Use of tracer injections and synoptic sampling to measure metal loading from acid mine drainage: U.S. Geological Survey Fact Sheet 245–96, 4 p.

Kimball, B.A., Bencala, K.E., and Runkel, R.L., 2000, Quantifying effects of metal loading from mine discharge, *in* Fifth

International Conference on Acid Rock Drainage, Denver, 2000, Proceedings: v. II, ICARD 2000, p. 1381–1390.

Kimball, B.A., Broshears, R.E., Bencala, K.E., and McKnight, D.M., 1994, Coupling of hydrologic transport and chemical reactions in a stream affected by acid mine drainage: Environmental Science & Technology, v. 28, p. 2065–2073.

Kimball, B.A., Runkel, R.L., Bencala, K.E., and Walton-Day, Katherine, 1999, Use of tracer-injection and synoptic-sampling studies to quantify effects of metal loading from mine drainage, *in* Morganwalp, D.W., and Buxton, H.T., eds., U.S. Geological Survey Toxic Substances Hydrology Program—Proceedings of the Technical Meeting, Charleston, South Carolina, March 8-12, 1999, Volume 1—Contamination from hardrock mining: U.S. Geological Survey Water-Resources Investigations Report 99–4018A.

Knauth, L.P., and Greenbie, M., 1997, Stable isotope investigation of ground-water surface-water interactions in the Verde River headwaters area: Arizona State University Department of Geology report in fulfillment of Arizona Water Protection Fund Grant #95-001, administered by Arizona Department of Water Resources, 28 p.

Krieger, M.H. 1965, Geology of the Prescott and Paulden quadrangles, Arizona: U.S. Geological Survey Professional Paper 467, 127 p.

Long, H.K. and Farrar, J.W., 1995, Report on the U.S. Geological Survey's evaluation program for standard reference samples distributed in May 1995—T-135 (trace constituents), M-134 (major constituents), N-45 (nutrients), N-46 (nutrients), P-24 (low ionic strength), Hg-20 (mercury), and SED-5 (bed material): U.S. Geological Survey Open-File Report 95–395, 135 p.

MacCormack, H.F., Fisk, G.G., Duet, N.R., Evans, D.W., and Castillo, N.K., 2002, Water Resources Data, Arizona, Water Year 2001: U.S. Geological Survey Water-Data Report AZ-01–1, p. 257.

Muller, A.B., and Mayo, A.L., 1986, ^{13}C variation in limestone on an aquifer-wide scale and its effects on groundwater ^{14}C dating models: Radiocarbon, v. 28, no. 3., p. 1041–1054.

Owen-Joyce, S.J., and Bell, C.K., 1983, Appraisal of water resources in the Upper Verde River area, Yavapai and Coconino Counties, Arizona: Arizona Department of Water Resources Bulletin 2, 219 p.

Parkhurst, D.L., and Plummer, L.N, 1993, Geochemical models, *in* regional ground-water quality: Chapter 9 *of* Alley, W.M., ed., Van Nostrand Reinhold, New York, p. 199–225.

Parkhurst, D.L., and Appelo, C.A.J., 1999, User's guide to PHREEQC (Version 2)—A computer program for speciation, batch-reaction, one-dimensional transport, and inverse geochemical calculations. U.S. Geological Survey Water-Resources Investigations Report 99–4259, 312 p.

Plummer, L.N., Prestemon, E.C., and Parkhurst, D.L., 1994, An interactive code (NETPATH) for modeling NET

geochemical reactions along a flowpath, version 2.0: U.S. Geological Survey Water-Resources Investigations Report 94–4169, 130 p.

Rantz, S.E, (compiler), 1982, Measurement and Computation of Streamflow—v. 1, Measurement of stage; v. 2, Computation of discharge: U.S. Geological Survey Water-Supply Paper 2175, v. 1, 284 p.; v. 2, 346 p.

Shelton, L.R., 1994, Field guide for collecting and processing of stream-water samples for the National Water-Quality Assessment Program: U.S. Geological Survey Open-File Report 94-455, 42 p.

Tadayon, Saeid, Duet, N.R., Fisk, G.G., MacCormack, H. F., Partin, C.K., Pope, G.L., and Rigas, P.D., 2001, Water Resources Data, Arizona, Water Year 2000: U.S. Geological Survey Water-Data Report AZ-00–1, p. 250.

Tadayon, Saeid, Duet, N.R., Fisk, G.G., MacCormack, H. F., Partin, C.K., Pope, G.L., and Rigas, P.D., 2000, Water Resources Data, Arizona, Water Year 1999: U.S. Geological Survey Water-Data Report AZ-99–1, p. 225.

Walton-Day, Katherine, Runkel, R.L., Kimball, B.E., and Bencala, K.E., 1999, Application of the solute-transport models OTIS and OTEQ and implications for remediation in a watershed affected by acid mine drainage: Cement Creek, Animas River Basin, Colorado, *in* Morganwalp, D.W., and Buxton, H.T., eds., U.S. Geological Survey Toxic Substances Hydrology Program—Proceedings of the Technical Meeting, Charleston, South Carolina, March 8-12, 1999: Volume 1—Contamination from hardrock

mining: U.S. Geological Survey Water-Resources Investigations Report 99-4018A.

Wilde, F.D., Radtke, D.B., Gibs, Jacob, and Iwatsubo, R.T. (eds.), 1999, National field manual for the collection of water-quality data: Techniques of Water Resources Investigations TWI 09-A4, book 9, chap. A6, sections 6.0, 6.0.1, 6.0.2, 6.0.2.A, and 6.0.2B, 152 p.

Wirt, Laurie, and Hjalmarson, H.W., 2000, Sources of springs supplying base flow to the Verde River headwaters, Yavapai County, Arizona: U.S. Geological Survey Open-file Report 99–0378, 50 p.

Wirt, Laurie, Leib, Kenneth J., and Mast, M. Alisa, 2000, Chemical-constituent loads during thunderstorm runoff in a high-altitude alpine stream affected by acid drainage, *in* Fifth International Conference on Acid Rock Drainage, Denver, 2000, Proceedings: V. II, ICARD 2000, p. 1391–1401.

Wirt, Laurie, Leib, Kenneth J., Bove, Dana, and Melick, Roger, 2001, Metal loading assessment of point and nonpoint sources in a small alpine subbasin characterized by acid drainage—Prospect Gulch, upper Animas River watershed, Colorado: U.S. Geological Survey Open-File Report 01–0258, 36 p.

Zellweger, G.W., 1996, Tracer injections in small streams—why and how we do them, *in* Morganwalp, D.W., and Aronson, D.A., eds., U.S. Geological Survey Toxic Substances Hydrology Program—Proceedings of the Technical Meeting, Colorado Springs, Colo., September 20–24, 1993: U.S. Geological Survey Water-Resources Investigations Report 94–4015, v. 2, p. 765–768.